Bulletin of Mathematical Biology manuscript No.
(will be inserted by the editor)

Preytaxis and travelling waves in an eco-epidemiological model

Andrew M. Bate[1,2] **and Frank M. Hilker**[1,3]

Received:?October 28, 2018?/Accepted:date

Abstract

Preytaxis is the attraction (or repulsion) of predators along prey density gradients and a potentially important mechanism for predator movement. However, the impact preytaxis has on the spatial spread of a predator invasion or of an epidemic within the prey has not been investigated. We investigate the effects preytaxis has on the wavespeed of several different invasion scenarios in an eco-epidemiological system. In general, preytaxis cannot slow down predator or disease invasions and there are scenarios where preytaxis speeds up predator or disease invasions. For example, in the absence of disease, attractive preytaxis results in an increased wavespeed of predators invading prey, whereas repulsive preytaxis has no effect on the wavespeed, but the wavefront is shallower. On top of this, repulsive preytaxis can induce spatiotemporal oscillations and/or chaos behind the invasion front, phenomena normally only seen when the (non-spatial) coexistence steady state is unstable. In the presence of disease, the predator wave can have a different response to attractive susceptible and attractive infected prey. In particular, we found a case where attractive infected prey increases the predators' wavespeed by a disproportionately large amount compared to attractive susceptible prey since a predator invasion has a larger impact on the infected population. When we consider a disease invading a predator–prey steady state, we found some counter-intuitive results. For example, the epidemic has an increased wavespeed when infected prey attract predators. Likewise, repulsive susceptible prey can also increase the infection wave's wavespeed. These results suggest that preytaxis can have a major effect on the interactions of predators, prey and diseases.

1. Centre for Mathematical Biology, Department of Mathematical Sciences, University of Bath, Bath BA2 7AY, UK

2. Environment Department, University of York, Heslington, York YO10 5NG

3. Institute of Environmental Systems Research, School of Mathematics/Computer Science, Osnabrück University, Barbarastr. 12, 49076 Osnabrück, Germany

E-mail: andrew.bate@york.ac.uk

1 Introduction

For a species (or infection) to successfully invade, it must first be introduced, then establish locally and then spread (Petrovskii and Li, 2006), usually in the form of a travelling wave. There are many examples of predator invasions that are considered to have spread like a travelling wave. The Colorado potato beetle spread rapidly across mainland Europe during the mid 20th century (Johnson, 1967; Begon et al, 2002), damaging potato crops as it spread. Red foxes have spread across much of mainland Australia over the last 140 years after being introduced in south Victoria around 1871, with major impact on birds and medium-sized mammals (Dickman, 1996). Likewise, there are many epidemics that also moved like a travelling wave, from the Black Death during 14th Century Europe to the spread of rabies across continental Europe (Murray, 2003; Shigesada and Kawasaki, 1997; Langer, 1964, Chapter 13). Other famous invasions that have moved like travelling waves are the muskrat invasion of Europe (Skellam, 1951; Britton, 2003) and the grey squirrel invasion of the British Isles, which has had a massive impact on the native red squirrel (Middleton, 1930; Lloyd, 1983; Tompkins et al, 2003; Bell et al, 2009).

Most models that involve spatial movement assume that prey and predators (especially when using partial differential equations) move by diffusion only. This means that predators and prey move in a random manner with no bias or external stimuli. However, movement is often not random. In particular, there are many external factors that attract or repel prey and predators, be it chemical attractant/repellent gradients (chemotaxis), gradients of oxygen (aerotaxis) or gradients of prey density (preytaxis).

The term ‘preytaxis’ was first coined in Kareiva and Odell (1987), where they modelled movement patterns of foraging Ladybirds. There are two ways for modelling preytaxis, ‘direct’ and ‘indirect’ (Tyutyunov et al, 2017). Direct preytaxis involves incorporating a flux in the predator dynamics that is dependent on gradients of prey density (as used in Kareiva and Odell, 1987; Grünbaum, 1998; Lee et al, 2008, 2009; Ainseba et al, 2008), whereas indirect preytaxis involves incorporating a separate predator velocity equation where predators accelerate according to prey gradients (with some diffusion term to harmonise predator velocities with neighbours) (as used in Arditi et al, 2001; Sapoukhina et al, 2003; Chakraborty et al, 2007; Tyutyunov et al, 2017). In other words, direct preytaxis means the predators’ velocity is proportional to prey gradients (a formulation akin to other classical taxis models like chemotaxis), whereas indirect preytaxis means predators accelerate towards a velocity that is proportional to prey gradients.

These two different schools of modelling preytaxis seem to give different results. Direct preytaxis is found to have a stabilising effect, limiting spatiotemporal oscillations and chaos (Lee et al, 2009), whereas indirect preytaxis can only have a stabilising effect for intermediate values of (attractive) preytaxis, i.e. strong preytaxis can induce spatiotemporal chaos and oscillations (Sapoukhina et al, 2003). This difference may be attributed to the fact that there is some ‘inertia’ or delay with indirect preytaxis; when predators reach the peak of prey density they no longer accelerate but still have

velocity and thus can overshoot. In this paper, the direct, flux-based method for preytaxis, is used, largely because instantaneous velocity changes in predators seem to be a reasonable assumption that is relatively simple and tangible.

In previous preytaxis papers, the focus has largely been on pattern formation (Chakraborty et al, 2007; Ainseba et al, 2008; Lee et al, 2009) or on the effect preytaxis has for pest control (Sapoukhina et al, 2003; Lee et al, 2008). We are not aware of studies focusing on how preytaxis alters predator invasions, the corresponding travelling waves and their wavespeeds, although Ainseba et al (2008) found that predators with preytaxis and diffusion can fill a 2D domain faster than with diffusion alone.

We are also not aware of preytaxis papers that consider the impact a disease has on a preytactic predator–prey interaction, or the impact preytaxis has on disease dynamics. In fact, in eco-epidemiology, there are only a handful of papers including spatial interactions. Many of these spatial eco-epidemiological papers are motivated by infections within plankton communities (Malchow et al, 2004, 2005; Hilker et al, 2006; Sieber et al, 2007; Siekmann et al, 2008) or lynx-rabbit dynamics (Roy and Upadhyay, 2015; Upadhyay et al, 2016), whereas there are some on a general predator–prey–disease system (Su et al, 2008, 2009; Su and Hui, 2011; Ferreri and Venturino, 2013).

In this paper, we will develop a spatial eco-epidemiological model that incorporates the random (diffusive) movement of predators and prey as well as predators moving along susceptible and infected prey gradients (preytaxis). Following that, we will consider the results of various invasion scenarios, with a particular focus on how preytaxis affects the resulting travelling wave and its wavespeed.

2 Model derivation

Consider a model with susceptible prey, infected prey and predators, denoted by the densities s, i and p, respectively. Firstly, we will define the non-spatial parameters. Let b be the per-capita birth rate for prey and let m and d be the natural per-capita death rates for prey and predators, respectively. Let c be the coefficient for density dependent mortality caused by competition among prey, which results in logistic growth for the prey. We assume that infection does not alter the host's per capita birth rate b and competition coefficient c. β is the transmissibility of the disease (in this case, the transmissibility term for density-dependent transmission; we will later briefly consider frequency-dependent transmission). a_S and a_I are the attack rates of the predator on susceptible and infected prey, respectively. Likewise, h_S and h_I are the handling times of the predator when attacking susceptible and infected prey, respectively. μ is the additional per-capita disease-induced mortality for infected prey. And lastly, e is a conversion coefficient of predators from eating prey.

Now, we will assume that susceptible prey, infected prey and predators experience diffusion with coefficients D_S, D_I and D_P, respectively. In addition to diffusion, we assume that predators move by 'direct' preytaxis, which we assume

is proportional to prey gradients. This means that the preytaxis flux is $pF_S\frac{\partial s}{\partial x}$ and $pF_I\frac{\partial i}{\partial x}$ for susceptible and infected prey, respectively, where F_S and F_I are the preytaxis coefficients for predators following susceptible and infected prey, respectively. This form of preytaxis is chosen because it is a relatively simple form (as F_S and F_I are constants and not functions of S or I) that includes different preytaxis terms for infected and susceptible prey. The coefficients can be positive or negative; positive coefficients mean that predators are attracted to prey, whereas negative coefficients mean that predators are repelled by prey. Unless otherwise stated, all parameters are strictly positive.

$$\frac{\partial s}{\partial t} = D_S\frac{\partial^2 s}{\partial x^2} + b(s+i) - ms - cs(s+i) - \beta si - \frac{a_S sp}{1+a_S h_S s + a_I h_I i}, \tag{1}$$

$$\frac{\partial i}{\partial t} = D_I\frac{\partial^2 i}{\partial x^2} + \beta si - (m+\mu)i - ci(s+i) - \frac{a_I ip}{1+a_S h_S s + a_I h_I i}, \tag{2}$$

$$\frac{\partial p}{\partial t} = D_P\frac{\partial^2 p}{\partial x^2} - \frac{\partial}{\partial x}\left(pF_S\frac{\partial s}{\partial x} + pF_I\frac{\partial i}{\partial x}\right) + \frac{ep(a_S s + a_I i)}{1+a_S h_S s + a_I h_I i} - dp. \tag{3}$$

We will assume zero flux boundary conditions on the boundaries of spatial domain $[0,L]$, i.e. $\frac{\partial s}{\partial x}(0,t) = \frac{\partial s}{\partial x}(L,t) = 0$, $\frac{\partial i}{\partial x}(0,t) = \frac{\partial i}{\partial x}(L,t) = 0$ and $\frac{\partial p}{\partial x}(0,t) = \frac{\partial p}{\partial x}(L,t) = 0$ for all times t, where L is the length of the domain. Now, we non-dimensionalise to simplify and reduce the number of parameters. Let $t = \tau T$, $s = \gamma S$, $p = \delta P$ and $x = \chi X$. Then, we choose τ such that the non-dimensional per-capita predator death rate is one ($\tau = \frac{1}{d}$), χ such that the susceptible prey diffusion is set to one ($\chi^2 = \frac{D_S}{d}$), δ such that the coefficient of the numerator of the susceptible prey functional response (attack rate) becomes one ($\delta = \frac{d}{a_S}$) and γ such that the coefficient for susceptible prey predation in the predators' numerical response is set to one ($\gamma = \frac{d}{ea_S}$). Given this, we have:

$$\frac{\partial S}{\partial T} = \frac{\partial^2 S}{\partial X^2} + b'(S+I) - m'S - c'S(S+I) - \beta' SI - \frac{SP}{1+h'_S S + a_R h'_I I}, \tag{4}$$

$$\frac{\partial I}{\partial T} = D_R\frac{\partial^2 I}{\partial X^2} + \beta' SI - (m'+\mu')I - c'I(S+I) - \frac{a_R IP}{1+h'_S S + a_R h'_I I}, \tag{5}$$

$$\frac{\partial P}{\partial T} = D'_P\frac{\partial^2 P}{\partial X^2} - \frac{\partial}{\partial X}\left(PF'_S\frac{\partial S}{\partial X} + PF'_I\frac{\partial I}{\partial X}\right) + \frac{P(S+a_R I)}{1+h'_S S + a_R h'_I I} - P, \tag{6}$$

where $b' = \frac{b}{d}$, $m' = \frac{m}{d}$, $c' = \frac{c}{ea_S}$, $\beta' = \frac{\beta}{ea_S}$, $h'_S = \frac{dh_S}{e}$, $a_R = \frac{a_I}{a_S}$ (relative attack rate), $h'_I = \frac{dh_S}{e}$, $D_R = \frac{D_I}{D_S}$, $\mu' = \frac{\mu}{d}$, $D'_P = \frac{D_P}{D_S}$, $F'_S = \frac{dF_S}{ea_S D_S}$ and $F'_I = \frac{dF_I}{ea_S D_S}$. Likewise, from the spatial scaling, we have that $L' = \frac{L\sqrt{d}}{\sqrt{D_S}}$.

To simplify terminology, we will drop all the primes. Now, we will replace susceptible prey with a total prey class, $N = S + I$. Consequently, we have:

$$\frac{\partial N}{\partial T} = \frac{\partial^2 N}{\partial X^2} + (D_R - 1)\frac{\partial^2 I}{\partial X^2} + bN - mN - cN^2 - \mu I - \frac{(N + (a_R - 1)I)P}{1 + h_S N + (a_R h_I - h_S)I}, \tag{7}$$

$$\frac{\partial I}{\partial T} = D_R\frac{\partial^2 I}{\partial X^2} + \beta(N-I)I - (m+\mu)I - cIN - \frac{a_R IP}{1 + h_S N + (a_R h_I - h_S)I}, \tag{8}$$

$$\frac{\partial P}{\partial T} = D_P\frac{\partial^2 P}{\partial X^2} - \frac{\partial}{\partial X}\left(PF_S\frac{\partial N}{\partial X} + P(F_I - F_S)\frac{\partial I}{\partial X}\right) + \frac{P(N + (a_R - 1)I)}{1 + h_S N + (a_R h_I - h_S)I} - P. \tag{9}$$

To make analysis easier, we will gather terms. Let $f(N,I) = \frac{N+(a_R-1)I}{1+h_S N+(a_R h_I - h_S)I}$ (the functional response on all prey), $g(N) = b - m - cN$ (per capita growth rate of prey in absence of disease and predation), $k(N,I) = \beta(N-I) - (m+$

$\mu) - cN$ (per-capita net growth rate of infected prey in the absense of predation) and $f_I(N,I) = \frac{a_R}{1+h_S N+(a_R h_I - h_S)I}$ (the functonal response on infected prey). Then these equations can be written as:

$$\frac{\partial N}{\partial T} = \frac{\partial^2 N}{\partial X^2} + (D_R - 1)\frac{\partial^2 I}{\partial X^2} + Ng(N) - \mu I - f(N,I)P, \tag{10}$$

$$\frac{\partial I}{\partial T} = D_R \frac{\partial^2 I}{\partial X^2} + I(k(N,I) - f_I(N,I)P), \tag{11}$$

$$\frac{\partial P}{\partial T} = D_P \frac{\partial^2 P}{\partial X^2} - \frac{\partial}{\partial X}\left(PF_S \frac{\partial N}{\partial X} + P(F_I - F_S)\frac{\partial I}{\partial X}\right) + P(f(N,I) - 1). \tag{12}$$

The zero flux boundary conditions are $\frac{\partial N}{\partial X}(0,T) = \frac{\partial N}{\partial X}(L,T) = 0$, $\frac{\partial I}{\partial X}(0,T) = \frac{\partial I}{\partial X}(L,T) = 0$ and $\frac{\partial P}{\partial X}(0,T) = \frac{\partial P}{\partial X}(L,T) = 0$ for all time T. Also, for simplicity we will assume that susceptible and infected prey only differ by the inclusion of disease-induced mortality and different preytaxis coefficients (i.e. $a_R = 1$, $D_R = 1$ and $h_S = h_I$).

3 Non-spatial dynamics

Before we analyse the spatial dynamics, in particular the wavespeeds, we first have to get some basic understanding of the non-spatial dynamics. This is done by analysing the steady states and their stability in the absence of diffusion and prey-taxis.

- $(N^*, I^*, P^*) = (0,0,0)$. This always exists, and is stable if $g(0) < 0$, i.e. $b < m$.
- $(N^*, I^*, P^*) = (N^*, 0, 0)$, which satisfies $g(N^*) = 0$ $\left(\text{i.e. } N^* = \frac{b-m}{c}\right)$. This exists if $g(0) > 0$ (i.e. $b > m$), and is stable if $k(N^*,0) < 0$ $\left(\text{i.e. } R_0 = \frac{\beta N^*}{m+\mu+cN^*} < 1\right)$ and $f(N^*,0) < 1$ (i.e. $(b-m)(1-h_S) < c$)
- $(N^*, I^*, P^*) = (N^*, 0, P^*)$, which satisfies $f(N^*,0) = 1$ $\left(\text{i.e. } N^* = \frac{1}{1-h_S}\right)$ and $P^* = N^* g(N^*) = \frac{(b-m)(1-h_S)-c}{(1-h_S)^2}$. This exists if $h_S < 1$ and $(b-m)(1-h_S) > c$. This is stable if the disease can not establish in the presence of predators $\left(k(N^*,0) < P^* f_I(N^*,0), \text{ i.e. } R_0^P = \frac{\beta N^*}{m+\mu+cN^*+P^* f_I(N^*,0)} < 1\right)$ as well as $g(N^*) - cN^* - P^* \frac{\partial f(N^*,0)}{\partial N} < 0$. The latter condition is the result of a Hopf bifurcation at $g(N^*) - cN^* - P^* \frac{\partial f(N^*,0)}{\partial N} = 0$, and thus stable limit cycles are likely to occur if this condition is broken.
- $(N^*, I^*, P^*) = (N^*, I^*, 0)$, which satisfies $k(N^*, I^*) = 0$ $\left(\text{i.e. } I^* = N^*\left(1 - \frac{m+\mu+cN^*}{\beta N^*}\right)\right)$ and $N^* g(N^*) = \mu I^*$. This equation forms a quadratic in terms of N^*, which always has one positive and one negative solution. This exists if $0 < I^* < N^*$. It is stable when $f(N^*, I^*) < 1$.
- $(N^*, I^*, P^*) = (N^*, I^*, P^*)$, which satisfies $f(N^*, I^*) = 1$, $k(N^*, I^*) = f_I(N^*, I^*)P^*$ and $g(N^*) = \mu I^* + P^*$. This exists when $P^* > 0$ and $N^* > I^* > 0$. We have not investigated its stability, but understand that this steady state can lose its stability via a Hopf bifurcation.

It is important to note that, at most, only one steady state is stable. There is no bistability between steady states. This does not say anything about possible bistability involving cyclic and chaotic attractors (like those in Bate and Hilker,

2013a). If we assume that $a_R = 1$ and $h_S = h_I$, then the non-spatial model would be the same as Bate and Hilker (2014) but with a Holling Type II functional response instead of a Holling Type IV functional response.

4 Spatio-temporal dynamics

From this point on, we will consider the effect preytaxis has on various invasion scenarios; (1) predator invasion in the absence of infected prey, (2) predator invasion in the presence of infected prey and (3) disease invasion in the presence of predators, with a particular focus on the wavespeed of the resulting travelling wave invasion. We assume that the 'native' species are at their corresponding steady state (with parameter values chosen so that this is stable when ignoring spatial effects) everywhere in the spatial domain of [0,250], but we will introduce an invader as a step function with invader density of 0.1 for $x \in [0,20]$ and invader density of 0 elsewhere. In such invasion scenarios, the solutions converge over time to travelling waves.

In the Appendix, we find an analytic minimum wavespeed by looking for travelling wave solutions with constant wavespeeds. We use the transformation $Z = X - \omega T$ (where ω is the constant wavespeed), linearise ahead of the wave (i.e. at the native steady state) and look at the eigenvalues to see if there are any complex eigenvalues that would lead to unrealistic travelling waves (negative populations). This would be sufficient for finding the actual wavespeed if we have 'linear determinacy' (Lewis et al, 2002), i.e. linearising ahead of the travelling wave gives the wavespeed. In single species systems, it is sufficient for there to be no Allee effect (assuming a constant diffusion coefficient, Aronson and Weinberger, 1975, 1978; Shigesada and Kawasaki, 1997). Many systems have been shown to exhibit linear determinacy, but the theory for linear determinacy is lacking for multispecies systems (Bell et al, 2009), with a notable exception of competitive/cooperative systems (Lewis et al, 2002). Despite the lack of theory, analogous arguments to scalar systems (like linearising in front of the wave) provide a great deal of success in calculating the wavespeed (Malchow et al, 2008; Bell et al, 2009), i.e. linear determinacy has been shown to be true in many multispecies systems, usually numerically. However, this is not always true, there are cases where the actual wavespeed is substantially faster than the calculated minimum wavespeed (Hosono, 1998).

The minimum wavespeeds calculated in the Appendix are independent of preytaxis terms, since these wavespeeds are calculated at the leading edge of the invasion front (where the system is near the native steady state, with negligible gradients) which results in negligible preytaxis terms. In the absence of preytaxis, we expect that the travelling wave will form and will move at the minimum speed ω_{crit} (after some transient), since the initial condition has compact support (as the initial condition for the invader is zero beyond $x = 20$). Proving mathematically that the travelling wave moves at the minimum wavespeed is very difficult, even for simpler models (Edelstein-Keshet, 1988; Murray, 2003), but we can verify numerically that these wavespeeds are attained (after some transients).

We numerically solve the predator–total-prey–infected-prey system 10-12 using a Strang splitting scheme (Chapter 18 of LeVeque, 1992; Tyson et al, 2000), where the diffusion, preytaxis and local population growth terms are solved as separate steps with appropriate numerical routines (using a full timestep of midpoint method for local growth, sandwiched by two half-timesteps of (two-step) Lax–Wendroff for preytaxis and two half-timesteps of Crank–Nicolson for diffusion). This method overcomes issues around finding a single method that can deal with diffusion and preytaxis, simultaneously. A full discussion of the numerical methods used is available in the Appendix.

4.1 Predator invasion in the absence of infected prey

4.1.1 Without preytaxis ($F_S = 0$)

In the absence of preytaxis, we have a reaction–diffusion predator–prey model. Similar models have been analysed elsewhere (for example Murray, 2003). During the initial stages of the invasion, the dynamics are dominated by the predator establishing and growing locally at the expense of prey (Figure 1(a)). By the time $T = 5$, a wave front is largely established, with a predator–prey coexistent steady state behind the wave front and a prey-only steady state ahead of the wave. Figure 1(b) demonstrates that the wave follows the 'moving line' (representing where the predator range starting from its initial distribution would be if it moved at the analytic minimum wavespeed), which tells us that the predator invasion wave is moving at the same speed as the analytically derived minimum speed ω_{crit}. Behind the wavefront, there are some dampened spatiotemporal oscillations. These oscillations are consistent with what would be expected since with the chosen parameter values, the predator–prey steady state is a stable focus.

4.1.2 With attractive preytaxis ($F_S > 0$)

Now, incorporating preytaxis into the predator–prey dynamics gives us a reaction–diffusion–taxis predator–prey model. First, let's consider attractive preytaxis, i.e. predators are attracted to places of high prey density.

At early stages, the populations are distributed similarly to the case without taxis, with Figure 2(a) looking nearly identical to Figure 1(a). However, over time, results change substantially. Whereas in Figure 1(b), we have that the wave travels at the same speed as the 'moving line', Figure 2(b) shows that the wave front overtakes the 'moving line', telling us that the travelling wave is moving at a speed significantly faster than the analytically derived minimum speed ω_{crit}. In other words, attractive preytaxis has increased the predator invasion wave speed.

To demonstrate this effect further, we have set predator diffusion $D_P = 0$ in Figure 3. By doing so, the analytic wavespeed of the predator wave is zero, which would suggest that the predator can only grow in regions in which it is

already established.[1] However, Figure 3 (and Figure 13, in Appendix) clearly has a travelling wave with constant positive wavespeed. This wavespeed is substantial too; without diffusion the travelling wave has moved to approximately $x = 195$ by $t = 100$ (about 175 spatial units ahead of the moving line), whereas with diffusion at $D_P = 1$ (Figure 2(b)), the wave moved to approximately $x = 245$ by $t = 100$ (only about 25 spatial units ahead of the moving line). Together, these wavespeeds suggest that increasing diffusion will reduce the effect of preytaxis, a phenomenon demonstrated further in Figure 4, where the increase in wavespeed from preytaxis largely disappears when diffusion is increased to $D_P = 2$. Presumably, the reduced impact of preytaxis on wavespeed due to increased diffusion is largely the result of diffusion flattening the wavefront, reducing prey gradients and thus the strength of preytaxis.

4.1.3 With repulsive preytaxis ($F_S < 0$)

In this subsection, we will assume that predators find (susceptible) prey repulsive and thus move down prey gradients. This assumption may not seem that realistic at first glance, although possible cases where it may occur are presented in the Discussion. However, the idea of repulsive infected prey seems more plausible, and the results in this subsection will help in understanding the results that include infected prey.

Figure 5(a) shows that by time $t = 5$, the predator distribution is far from uniform around the wavefront, especially as a spike in predator density (with a corresponding trough in prey density) is formed. The wavefront stabilises as time goes on (Figure 5(b)), and moves at the analytic wavespeed. Immediately behind the wave, some dampened oscillations take place, which is consistent with the fact that the predator–prey steady state is a stable focus in the absence of spatial effects. However, further behind the wavefront, some spatiotemporal oscillations and/or chaos appear. In this case, the predator–prey steady state is not actually stable once spatial effects are taken into account.

Why would repulsive preytaxis induce oscillations? Well, since the steady state is a focus (in the absence of spatial effects), we would expect some (damped) oscillations. Given the existence of damped oscillations, we can suppose there are spatial regions with (relatively) high predator density and (relatively) low prey density. In such regions, we expect both prey and predator densities to decline further, prey because of the large numbers of predators, and predators because of the lack of prey to sustain them. However, if nearby there are regions with higher prey densities and lower predator densities, then the predators would migrate into the high-predator–low-prey region. If this movement is strong enough to replenish the predators lost from lack of prey and diffusion, then the peak in predator density is sustained. A similar argument applies to the persistence of troughs in predator density.

[1] Actually, since the smoothed initial condition in Figure 3 has predators everywhere, a wave might form from growth alone, given enough time. However, we get the same wavespeed from a step function, which tells us that the travelling wave depends on preytaxis, and not just on the growth of the initial condition (Figure 13, in Appendix). The change to a smoothed initial condition was made because the numerical regime for preytaxis (Lax–Wendroff) leads to some dampened 'spikiness'.

So why is the wavespeed for repulsive preytaxis the same as the analytically derived wavespeed? Well, the wave can not be any slower, as the analytic wavespeed was calculated as a minimum wavespeed. But repulsive preytaxis could be expected to slow down the wave, by the same argument as attractive preytaxis speeding up the wave. We suspect that instead, repulsive preytaxis picks a travelling wave that would otherwise move faster than the minimum wavespeed and be unstable in the absence of repulsive preytaxis. In this case, the predator wavefront is much shallower, which has been associated with faster travelling waves before (Murray, 2002, page 446, shows this for the single-species Fisher model). A way of understanding why shallower waves are faster is that shallower waves have a larger spatial region where total population growth is large (regions both ahead and behind of the wavefront do not contribute much to the growth of the invading population), and thus should have a greater growth overall and thus a greater wavespeed. The repulsive preytaxis slows down this shallower, faster wave to the analytic minimum wavespeed.

4.2 Predator invasion in the presence of infected prey

4.2.1 With attractive preytaxis

Earlier, we demonstrated that attractive preytaxis in the disease-free case can increase substantially the wavespeed for a predator invasion. However, looking at the simulation in Figure 6(a), if susceptibles attract predators, then the wavespeed[2] is only slightly increased in comparison to the case without preytaxis, despite the fact that susceptibles are much more attractive here than earlier in Figure 2. However, if infected prey attract predators, like in Figure 6(b), then the wavespeed of the predator invasion is substantially faster than both the travelling waves for no preytaxis and for attractive susceptible prey. Well, how can this be explained? We suspect that this phenomenon is related to the effect the predator has on each prey class. The effect of the predator on susceptible prey is that they are reduced by predation. However, infected prey take a much greater hit; not only do they experience the additional predation like susceptible prey, but also there are fewer susceptible prey to infect. Consequently, an invasion of predators has a much greater effect on infected prey; a result that is general for such models where predators do not discriminate between susceptible and infected prey (Packer et al, 2003), since Equations 10-12 are equivalent to exploitative competition ‘in disguise’ between predators and disease prevalence (Sieber and Hilker, 2011). This means that the gradient of infected prey is steep, whereas the susceptible prey gradient is considerably shallower (the changes in total prey density is largely explained by the changes in infected prey density). Consequently, infected prey have steeper gradients and thus a greater preytaxis effect than the shallower gradients of susceptible prey.

[2] Like we had without the disease; with no preytaxis, predators invade an endemic steady state as a travelling wave with the analytic minimum wavespeed (not shown).

4.2.2 With repulsive preytaxis

Figure 7(a) and (b) show that repulsive preytaxis does not slow the wave for repulsive susceptible and infected prey, respectively. However, the predator wave in Figure 7(b) is much shallower than the predator waves in Figure 6 (and is also much shallower than when there is no preytaxis). This suggests a similar phenomenon to what happened without the disease, namely that repulsive preytaxis can lead to shallower wavefronts. However, since the wave is not as shallow in Figure 7(a) as it is in Figure 7(b), we can conclude that infected prey can have a stronger repulsive preytaxis effect than susceptible prey. This is for the same reasons too, i.e. the wavefront has a much larger infected prey gradient since predators have a bigger impact on the infected prey class. Also, just as we had in the absence of the disease, repulsive preytaxis can lead to spatiotemporal oscillations and/or chaos.

4.3 Disease invasion in the presence of predators

If the predator does not exhibit preytaxis, then the disease spreads at the same speed as the analytic minimum wavespeed as the travelling wave follows the moving line (Figure 8). It is worth noting that because of the presence of predators, it is harder for a disease to become endemic, due to both the additional deaths of infected prey from predation and the reduced susceptible prey density from such predation. Consequently, a significant increase of transmissibility is needed for the disease to establish. Additionally, the invasion of the disease (once fully established locally) does not change the prey density as prey density is the same in front of and behind the disease invasion wavefront, and instead the predator density has been reduced. This reduction in predator density is consistent with the idea that the predator and disease are exploitative competitors (Hardin, 1960).

4.3.1 With attractive preytaxis

Now we consider that predators are attracted to susceptible prey. Since it is the disease that is invading and not the predator, there is no direct intuition that would suggest that preytaxis would change the wavespeed, and this is what we find in Figure 9(a), as the travelling wave follows the 'moving line'. Now, suppose that infected prey attract predators. Here we find that preytaxis can have an impact on the wavespeed, although this impact seems weak. For example, in Figure 9(b), the disease wave has just about overtaken the 'moving line', despite the attractive strength of preytaxis being particularly large ($F_I = 20$). The suspected reason for the increased wavespeed is as follows. Once a disease epidemic wavefront is formed, predators would move up the wavefront resulting in a trough in predator density just ahead of the wave and a peak of predator density just behind the wavefront. Having a reduced predator density directly in front of the wave means that (susceptible) prey density is higher. Combining these two effects (their relative importance is not

known), the infected prey can spread a little faster since there are more susceptibles to infect as well as a reduced death rate from the reduction in predator density just ahead of the wavefront.

4.3.2 With repulsive preytaxis

Figure 10 demonstrates some interesting results that occur when susceptible prey repel predators. In Figure 10(a), the disease wave is moving faster than the analytic wavespeed, with oscillations in the tail.

Why is this wave faster than expected? As we have seen in the predator invasion with repulsive preytaxis (Figure 5(b)), the system can be oscillatory/chaotic. In Figure 10(a), the presence of an infection seems to perturb the predator–prey steady state, resulting in such oscillations and chaos. We will call these oscillations and chaos within the predator–susceptible-prey system 'turbulence', a 'turbulence' that spreads over time at its own speed. In the turbulence, we have that predator density is on average smaller than at the steady state, and total prey density is on average higher than at the steady state (akin to $\overline{N} > N^*$ and $\overline{P} < P^*$ described in Bate and Hilker (2013b) and Armstrong and McGehee (1980)). If the turbulence is moving fast enough to 'escape' the disease (as is the case in Figure 10(a)), the assumption of a predator–prey steady state ahead of the infection wave for the analytic wavespeed is no longer valid, and instead the infection wavespeed should be based on the (probably average) densities of the turbulence ahead of the wave.

Now suppose that the disease has frequency-dependent transmission and compare Figure 10(b) with Figure 10(a). Figure 10(b) shows the same turbulence as Figure 10(a). However, the disease wave moves only at the analytic wavespeed and no faster; the turbulence does not speed up the wave. The lack of an increased wavespeed in turbulence supports the idea that the increase in wavespeed in Figure 10(a) is due to the change in the average predator and prey densities in the turbulence, as it is reminiscent of results in Bate and Hilker (2013b). In Bate and Hilker (2013b), it was found that the endemic thresholds for predator-prey steady states and (temporal) oscillations are different for density-dependent transmission but are the same for frequency-dependent transmission.

Back to density-dependent transmission, if we increase transmissibility from $\beta = 1$ (Figure 10(a)) to $\beta = 1.2$ (Figure 11), then there are no oscillations in the tail and the wavespeed is not faster than the infected prey. Instead, there is a pulse in prey density around the disease invasion wavefront, but prey density behind the wavefront is the same as ahead of the wavefront. Firstly, the disappearance of oscillations is probably the result of the increase in the infected prey population from the increase in transmissibility, which increases the total mortality of the total prey class. This additional mortality is known to stabilise Rosenzweig–MacArthur predator–prey oscillations (Hilker and Schmitz, 2008, and references therein). It also restricts the susceptible population, probably flattening susceptible prey gradients, and thus reducing the strength of preytaxis. Likewise, increasing transmissibility from $\beta = 1$ to $\beta = 1.2$ increases the analytical wavespeed, resulting in the infection wave being fast enough to keep up with the turbulence, and stabilises it. In such a case, there is no turbulent 'pull' and the wavespeed is the same as the analytic wavespeed.

Figure 12 considers the case where infected prey repel predators. The wavespeed is the same as the analytic wavespeed, i.e. the repulsive preytaxis does not speed up or slow down the travelling wave. In the tail behind the wave, there is a short window where the system is near the coexistent steady state before there is a shift to a regime of spatiotemporal oscillations/chaos in the wake of the travelling wave, a phenomenon already seen for repulsive preytaxis for predator invasions.

5 Discussion and conclusions

In this paper, we analysed the wavespeed of various invasion scenarios in a susceptible-prey–infected-prey–predator system and investigated the effect preytaxis has on the wavespeed of these invasions. In the absence of preytaxis, the wavespeed of the travelling wave is the same as the analytical minimum wavespeed. Adding preytaxis does not necessarily change the travelling wave's wavespeed. However, there are many cases where preytaxis increases the wavespeed for predator and disease invasion waves. An overall summary of our results is given in Table 1.

On the one hand, attractive preytaxis increases the wavespeed for a predator invasion into a prey population, a phenomenon found in Ainseba et al (2008). In particular, we found a preytaxis-induced wave where there would be no wave due to no predator diffusion in the absence of preytaxis. On the other hand, repulsive preytaxis does not seem to slow down the predator invasion wavespeed. The suspected reason for this is that the analytically derived wavespeed is a minimum speed for a travelling wave to exist (although some transient waves can be slower; Hastings, 1996). This is counter-intuitive as we expect repulsive preytaxis to slow down travelling waves. We suspect that this difference can be resolved if we consider that the shape of the wave would be that of a faster, shallower wave that is unstable when there is no preytaxis, but the preytaxis slows down this wave and makes it the stable wave (Murray, 2002, Chapter 13, especially page 446 and Figure 13.3, suggests that faster waves are shallower, at least for the Fisher model).

On top of the impact on the wavespeed, we found that repulsive preytaxis has a destabilising effect, creating and exacerbating predator–prey oscillations which do not exist in the absence of preytaxis. For example, we found many scenarios where, in the absence of spatial effects, the predator–prey steady state is stable, but with spatial effects, the predator–prey steady state is unstable and instead spatiotemporal oscillations and/or chaos are the dominant dynamics. This phenomenon was also recently found in Wang and Yang (2017), and we demonstrate analytically in the Appendix that repulsive preytaxis can destabilise an otherwise stable steady state. In the context of travelling waves, the oscillations resemble convective instability (Sherratt et al, 2014; Dagbovie and Sherratt, 2014, and references therein). In particular, there are windows of dynamical stabilisation (Petrovskii and Malchow, 2000; Malchow et al, 2008), where there is some region behind the travelling wave where the (convectively) unstable predator–prey steady state appears to be stable. Dynamical stabilisation usually occurs with convective instability where the instability moves more slowly than the

travelling wave. (If convective instability can be confirmed, to our knowledge, this would be the first case of convective instability where the steady state is stable when only considering the underlying kinetic ODEs.)

In this paper, we demonstrate that the impact of a disease can be considerable, with preytactic effects being considerably stronger for infected prey and considerably weaker for susceptible prey since predator populations have a disproportionate impact on infected prey population densities and little impact on susceptible prey population densities. Likewise, the consequences of preytaxis on a disease epidemic can lead to faster than expected epidemic wavespeeds if either infected prey are attractive for predators or when susceptible prey are sufficiently repulsive for spatio-temporal oscillations to occur and the disease transmissibility is density dependent and sufficiently weak to allow the spatio-temporal oscillations to outpace the disease wave. The former is due to predators being attracted away from the tip of the wavefront, whereas the latter is suspected to be due to the differences in average prey density in the spatio-temporal oscillations (akin to Bate and Hilker, 2013b).

5.1 Preytaxis and model assumptions

Here, we have assumed direct preytaxis where preytaxis coefficients are constant. This is the simplest assumption to make, and has been used elsewhere (Grünbaum, 1998; Lee et al, 2009), but other choices of taxis can be made. For example, Lee et al (2009) also consider $F_S \to \frac{F_S}{S}$, the same form as that in the chemotactic model (Keller and Segel, 1971). Lee et al (2008) adapted this by using $\frac{F_S}{S+\tau}$ and $\frac{F_S}{(S+\tau)^2}$ (which was also suggested for chemotaxis by Tyson et al, 1999), to avoid the singularity around $S = 0$. Ainseba et al (2008) did not give an explicit form for the preytaxis, but assumed that there is no preytaxis once prey density is above some threshold.

The choice of preytaxis terms focuses on the gradient of prey density. But surely the predator would benefit most from moving towards areas that maximise growth. This means preytaxis would be based on the gradient of the functional response and not of prey density. In fact, there are many cases discussed in Bate and Hilker (2014), where moving towards regions of high prey density would be a bad strategy for predators due to group defence. Additionally, if preytaxis is linked to numerical response gradients, then differences between handling times or attack/search rates for susceptible and infected prey (e.g. from infected prey being easier to catch) would also affect the strength of preytaxis.

We have only considered preytaxis, the movement of predators towards or away from prey. However, prey could also find predators repulsive or attractive. In fact, in Murray (2003, Chapter 1), such spatial systems are described as 'pursuit and evasion', suggesting prey movement is equally important to predator movement in predator–prey interactions. But preytaxis only considers whether predators actively pursue prey. It is very reasonable to consider prey evading predators or 'predataxis' (Berleman et al, 2008). It is usually in the prey's interest to avoid predators. For example, white-tailed deer tend to gather in between wolf pack territories (Murray, 2003, Chapter 14). Likewise, there are many predators that

attract prey using chemical, light or other effects. Angler fish attract prey with light and pitcher plants attract flies using their distinctive smell. Including predataxis could lead to other interesting (and possibly counter-intuitive) results. For example, given that attractive infected prey in an infection wave increase the infection's wavespeed, then a repulsive predator wave (i.e. repulsive predataxis) should lead to a gathering of prey just ahead of the predator wave, leading to an increased predator wavespeed. However, such predataxis could also be dependent on the predation pressure itself and not just on the number of predators. This means that prey have safety in numbers as they saturate the predator's functional response, at least until predator density increases from movement and growth.

In this paper, we explored the interaction of infected prey and preytaxis. Although to our knowledge this is a novel idea, there are several reasons why we might expect the infection of prey to influence predator movement. For many predators, predation on infected prey can be beneficial, even in several cases with trophic-transmitted diseases (Lafferty, 1992). In particular, there is a prevailing view in ecology that predators capture disproportionately many sick, weak, injured, young or old individuals of prey (Errington, 1946; Slobodkin, 1968; Curio, 1976). Additionally, many parasites alter the behaviour or appearance of their host that would make predation more likely (Dobson, 1988; Moore, 2002). For example, infection of mosquitofish (*Gambusia holbrooki*) by the nematode *Eustrongylides ignotus* lead to aberrant behaviour including lethargy, convulsions, and buoyancy abnormalities, resulting that infected prey were selected preferentially by predatory fishes (Coyner et al, 2001), whereas red grouse infected with *Trichostrongylus tenuis* emit stronger scents that make it easier for predators to find (Hudson et al, 1992). Conversely, *Toxoplasma gondii*-infected rats become fearless and attracted to feline urine (Berdoy et al, 2000; Vyas et al, 2007), which could be considered infection-induced attractive predataxis.

Repulsive preytaxis seems to be the cause for much of the interesting dynamics in this paper (like pattern formation and increased epidemic wavespeeds), but the concept of repulsive preytaxis might seem counter-intuitive. Repulsive infected prey are easier to give examples of. Predators may wish to avoid infected prey for the unpleasant taste, sight or smell. Predators may also fear of getting sick from eating prey. This is particularly likely with pathogens and parasites that are trophically transmitted (Lafferty, 1992). This does require infected prey to be distinguishable from susceptibles from a distance, or at least for predators to gain a sense of the density of infected prey from a distance. If susceptible and infected prey are indistinguishable for predators, the experience of meeting infected prey may put predators off prey in general, and thus susceptible prey may also become repulsive.

It may seem difficult to understand a predator finding susceptible prey repulsive (in the absence of disease). However, the repulsiveness of susceptible prey could be a variety of defence mechanisms. Such mechanisms could be forms of group defence (discussed in Krause and Ruxton, 2002; Freedman and Wolkowicz, 1986; Bate and Hilker, 2014). Many group defence mechanisms influence the functional response, e.g. by increasing the handling time due to predator confusion. In addition to functional response effects, there are possibly several other mechanisms for repulsive prey.

	Attractive susceptible prey	Repulsive susceptible prey	Attractive infected prey	Repulsive infected prey
Predators invading susceptible prey only	Figures 2, 3 & 13	Figure 5	N/A	N/A
... Wavespeed	Faster	Same	N/A	N/A
... Wavefront	Steeper	Shallower	N/A	N/A
... Spatio-temporal oscillations	No	Yes	N/A	N/A
Predators invading susceptible and infected prey	Figure 6a	Figure 7a	Figure 6b	Figure 7b
... Wavespeed	Faster? (weak)	Same	Faster	Same
... Wavefront	Steeper	Shallower	Steeper	Shallower
... Spatio-temporal oscillations	No	Yes	No	Yes
Disease invading predator–prey system	Figure 9a	Figure 10 & 11	Figure 9b	Figure 12
... Wavespeed	Same	Sometimes faster	Faster	Same
... Wavefront	Steeper?	Steeper	Steeper	Shallower
... Spatio-temporal oscillations	No	Yes	No	Yes

Table 1 Summary of key results, relative to the baseline case of no preytaxis.

For example, predators may fear getting mobbed from large groups of prey or prey may expel repellent chemicals or sounds. (Most of these repellents are reactive; passively spreading repellent chemicals is largely for sessile species like plants, corals and sponges, Kubanek, 2009, .) Additionally, prey could potentially alter the environment to something uncomfortable for predators; for example, prey might attract enemies of the predator that the predator would seek to avoid, or perhaps a herbivore prey could change the density of foliage away from those preferred by the predator. It is also worth noting that for predator invasion, the predator (and prey) may be naive to each other, although this argument does fall down if the time for the travelling wave to form and spread is at a comparable or slower time-scale than the time needed for the naivety to disappear.

In the presence of infection, predators may prefer moving towards regions of high infected prey densities as infected prey are often weaker and more vulnerable. Likewise, infected prey may attract predators if the infection is trophically transmitted. In such cases, repulsive susceptible prey can be understandable as predators find them difficult to overcome, whereas infected prey would attract predators.

In conclusion, we have found that by including preytaxis in an eco-epidemiological model, we can find many cases where preytaxis increases the wavespeed of predator and disease invasions. Preytaxis can also change the shape of the travelling wave and cause some spatiotemporal oscillations and/or chaos, but preytaxis has not been found slow down predator and disease invasions.

A Analytic minimum wavespeeds

To find analytical minimum wavespeeds, we need to assume there is a travelling wave solution with constant wavespeed, with a native steady state ahead of the wave and a coexisting steady state behind the wave. By doing so, we use the transformation $Z = X - \omega T$ (where ω is the constant wavespeed) to arrive at a system of ODEs. After linearising ahead of the wave (i.e. at the native steady state) we look at the eigenvalues to see if there are any complex eigenvalues that would lead to unrealistic travelling waves (i.e. negative populations), and consequently find conditions on the wavespeed.

A.1 Calculating for minimum wavespeeds

For travelling waves, we will seek solutions of the form $(N(X,T), I(X,T), P(X,T)) = (N(Z), I(Z), P(Z))$, where $Z = X - \omega T$ and ω is the wavespeed. We will also assume, for theoretical purposes, that the spatial domain is infinite. This is not a big assumption since the spatial domain is much larger than the wave itself. Likewise, we have assumed that $D_R = 1$. With this, the PDEs in equations (10)-(12) become:

$$-\omega\frac{dN}{dZ} = \frac{d^2N}{dZ^2} + Ng(N) - \mu I - f(N,I)P, \tag{13}$$

$$-\omega\frac{dI}{dZ} = \frac{d^2I}{dZ^2} + I(k(N,I) - f_I(N,I)P), \tag{14}$$

$$-\omega\frac{dP}{dZ} = D_P\frac{d^2P}{dZ^2} - \frac{d}{dZ}\left(PF_S\frac{dN}{dZ} + P(F_I - F_S)\frac{dI}{dZ}\right) + P(f(N,I) - 1). \tag{15}$$

Equations (13)-(15) can be rewritten as a system of six first order ODEs,

$$\frac{dN}{dZ} = \dot{N}, \tag{16}$$

$$\frac{d\dot{N}}{dZ} = -\omega\dot{N} - (Ng(N) - \mu I - Pf(N,I)), \tag{17}$$

$$\frac{dI}{dZ} = \dot{I}, \tag{18}$$

$$\frac{d\dot{I}}{dZ} = -\omega\dot{I} - I(K(N,I) - Pf_I(N,I)), \tag{19}$$

$$\frac{dP}{dZ} = \dot{P}, \tag{20}$$

$$\begin{aligned}\frac{d\dot{P}}{dZ} &= \frac{-1}{D_P}\left(\omega\dot{P} + P(f(N,I) - 1) - \left(F_S\left(\dot{P}\dot{N} + P\frac{d\dot{N}}{dZ}\right) + (F_I - F_S)\left(\dot{P}\dot{I} + P\frac{d\dot{I}}{dZ}\right)\right)\right) \\ &= \frac{-1}{D_P}[\dot{P}(\omega - F_S\dot{N} - (F_I - F_S)\dot{I}) + P(f(N,I) - 1)... \\ &\quad ... - P[F_S[-\omega\dot{N} - (Ng(N) - \mu I - Pf(N,I))]... \\ &\quad ... + (F_I - F_S)[-\omega\dot{I} - I(K(N,I) - Pf_I(N,I))]]].\end{aligned} \tag{21}$$

Without any preytaxis ($F_S = F_I = 0$), equation (21) becomes:

$$\frac{d\dot{P}}{dZ} = \frac{-1}{D_P}(\omega\dot{P} + P(f(N,I) - 1)).$$

The Jacobian for equations (16)-(21) (including preytaxis) is:

$$\begin{bmatrix}
0 & 1 & 0 & \cdots \\
-g(N) - N\frac{\partial g(N)}{\partial N} + P\frac{\partial f(N,I)}{\partial N} & -\omega & \mu & \cdots \\
0 & 0 & 0 & \cdots \\
-I\left(\frac{\partial K(N,I)}{\partial N} - P\frac{\partial f_I(N,I)}{\partial N}\right) & 0 & -(K(N,I) - Pf_I(N,I)) - I\left(\frac{\partial K(N,I)}{\partial I} - P\frac{\partial f_I(N,I)}{\partial I}\right) & \cdots \\
0 & 0 & 0 & \cdots \\
\frac{-P}{D_P}\left(\frac{\partial f}{\partial N}(N,I) + F_S\left(g(N) + N\frac{\partial g(N)}{\partial N} - P\frac{\partial f(N,I)}{\partial N}\right)\right. & \frac{-F_S}{D_P}(\omega P - \dot{P}) & \frac{-P}{D_P}\left(\frac{\partial f}{\partial I}(N,I) + F_S\left(\mu + \frac{\partial f}{\partial I}(N,I)\right) + (F_I - F_S)\left((K(N,I) - Pf_I(N,I))\right.\right. & \cdots \\
\left.\left. + (F_I - F_S)I\left(\frac{\partial K(N,I)}{\partial N} - P\frac{\partial f_I(N,I)}{\partial N}\right)\right) & & \left.\left. + I\left(\frac{\partial K(N,I)}{\partial I} - P\frac{\partial f_I(N,I)}{\partial I}\right)\right)\right)
\end{bmatrix}$$

$$\begin{bmatrix}
\cdots\ 0 & 0 & 0 \\
\cdots\ 0 & f(N,I) & 0 \\
\cdots\ 1 & 0 & 0 \\
\cdots\ -\omega & If_I(N,I) & 0 \\
\cdots\ 0 & 0 & 1 \\
\cdots\ \frac{-(F_I - F_S)}{D_P}(\omega P - \dot{P}) & \frac{-1}{D_P}(f(N,I) - 1 + F_S[\omega\dot{N} + (Ng(N) - \mu I - 2Pf(N,I))] & \frac{-1}{D_P}(\omega - F_S\dot{N} \\
 & \left. + (F_I - F_S)[\omega\dot{I} + I(K(N,I) - 2Pf_I(N,I))]\right) & -(F_I - F_S)\dot{I})
\end{bmatrix}$$

A.1.1 Predator invasion in the absence of infected prey

Consider that there is a prey-only steady state in front of a travelling wave of predators (thus we will ignore all infected prey equations/terms). We can linearise around this steady state, $(N, \dot{N}, P, \dot{P}) = (N^*, 0, 0, 0)$, where $g(N^*) = 0$, and ignore the disease, to get the Jacobian:

$$\begin{pmatrix}
0 & 1 & 0 & 0 \\
cN^* & -\omega & \mu & 0 \\
0 & 0 & 0 & 1 \\
0 & 0 & -\frac{f(N^*,0)-1}{D_P} & -\frac{\omega}{D_P}
\end{pmatrix}$$

Fortunately, this Jacobian is block upper triangular, so the eigenvalues are the eigenvalues of $\begin{pmatrix} 0 & 1 \\ cN^* & -\omega \end{pmatrix}$ and $\begin{pmatrix} 0 & 1 \\ -\frac{f(N^*,0)-1}{D_P} & -\frac{\omega}{D_P} \end{pmatrix}$. The former has eigenvalues $\frac{-\omega \pm \sqrt{\omega^2 + 4cN^*}}{2}$, which are always real, whereas the latter has eigenvalues $\frac{-\omega \pm \sqrt{\omega^2 - 4D_P(f(N^*,0)-1)}}{2D_P}$, which are real as long as $\omega \geq 2\sqrt{D_P(f(N^*,0) - 1)}$. This means that the travelling wave has a wavespeed of at least $\omega_{crit} = 2\sqrt{D_P(f(N^*,0) - 1)}$, a minimum wavespeed that is the actual wavespeed if we assume 'linear determinacy'. It is worth noting that this is independent of the preytaxis coefficients (F_S and F_I). The reason for this is that at the leading edge of the predator invasion, prey density is nearly constant and thus there is no prey gradient for preytaxis to occur. However, this does not mean that preytaxis will have no effect on the wave away from the front edge.

A.1.2 Predator invasion in the presence of susceptible and infected prey

Starting with the steady state $(N,\dot{N},I,\dot{I},P,\dot{P}) = (N^*,0,I^*,0,0,0)$, where $N^*g(N^*) = \mu I^*$ and $K(N^*,I^*) = 0$, the Jacobian becomes:

$$\begin{pmatrix} 0 & 1 & 0 & 0 & 0 & 0 \\ -g(N^*)+cN^* & -\omega & \mu & 0 & f(N^*,I^*) & 0 \\ 0 & 0 & 0 & 1 & 0 & 0 \\ -I^*\frac{\partial K(N^*,I^*)}{\partial N} & 0 & -I^*\frac{\partial K(N^*,I^*)}{\partial I} & -\omega & I^*f_I(N^*,I^*) & 0 \\ 0 & 0 & 0 & 0 & 0 & 1 \\ 0 & 0 & 0 & 0 & \frac{-1}{D_P}(f(N^*,I^*)-1) & \frac{-\omega}{D_P} \end{pmatrix}$$

Again, this is block upper-triangular, and thus we get the subsystem $\begin{pmatrix} 0 & 1 \\ -\frac{f(N^*,I^*)-1}{D_P} & -\frac{\omega}{D_P} \end{pmatrix}$. This has eigenvalues $\frac{-\omega\pm\sqrt{\omega^2-4D_P(f(N^*,I^*)-1)}}{2D_P}$. This means that the travelling wave has a wavespeed of at least $\omega_{crit} = 2\sqrt{D_P(f(N^*,I^*)-1)}$, which is the wavespeed assuming 'linear determinacy'.

The rest of the system is:

$$\begin{pmatrix} 0 & 1 & 0 & 0 \\ -g(N^*)+cN^* & -\omega & \mu & 0 \\ 0 & 0 & 0 & 1 \\ -(\beta-c)I^* & 0 & \beta I^* & -\omega \end{pmatrix}$$

This subsystem has eigenvalues $\lambda = \frac{-\omega\pm\sqrt{\omega^2-2(A\pm\sqrt{A^2-4B})}}{2}$, where $A = g(N^*)-cN^*-\beta I^* < 0$ and $B = I^*(\beta(\mu + cN^*-g(N^*))-c\mu) > 0$ (these are the trace and determinant of the Jacobian of the susceptible-infected prey subsystem around the endemic steady state, and $A^2-4B < 0$ is the condition for the steady state to be a stable focus). These eigenvalues, however, can have complex parts since $N^*,I^* > 0$, and thus a focus around (N^*,I^*) can be realistic (i.e. no issue about negative populations) and consequently this subsystem should not pose a restriction on the wave speed.

A.1.3 Disease invasion in the presence of predators

Here, we start with the steady state $(N,\dot{N},I,\dot{I},P,\dot{P}) = (N^*,0,0,0,P^*,0)$, where $f(N^*,0) = 1$ and $P^* = N^*g(N^*)$ (and assuming $g(N^*)-cN^*-P^*\frac{\partial f(N^*,0)}{\partial N} < 0$ for the steady state to be stable). Then the Jacobian becomes:

$$\begin{pmatrix} 0 & 1 & 0 & 0 & 0 & 0 \\ -g(N^*)+cN^*+P^*\frac{\partial f(N^*,0)}{\partial N} & -\omega & \mu & 0 & 1 & 0 \\ 0 & 0 & 0 & 1 & 0 & 0 \\ 0 & 0 & -(K(N^*,0)-P^*f_I(N^*,0)) & -\omega & 0 & 0 \\ 0 & 0 & 0 & 0 & 0 & 1 \\ \frac{-P^*}{D_P}\left(\frac{\partial f}{\partial N}(N^*,0)+F_S(g(N^*)-cN^*-P^*\frac{\partial f(N^*,0)}{\partial N})\right) & \frac{-F_S\omega P^*}{D_P} & \frac{-P^*}{D_P}\left(\frac{\partial f}{\partial I}(N^*,0)+F_S\left(\mu+\frac{\partial f}{\partial I}(N^*,0)\right)+(F_I-F_S)(K(N^*,0)-P^*f_I(N^*,0))\right) & \frac{(F_S-F_I)\omega P^*}{D_P} & \frac{F_SP^*}{D_P} & \frac{-\omega}{D_P} \end{pmatrix}$$

The middle two rows (for I and $\dot{I}$) can be separated as all other terms in these rows are zero. Thus we have the matrix $\begin{pmatrix} 0 & 1 \\ -(K(N^*,0)-P^* f_I(N^*,0)) & -\omega \end{pmatrix}$, which has the eigenvalues $\frac{-\omega \pm \sqrt{\omega^2 - 4(K(N^*,0)-P^* f_I(N^*,0))}}{2}$. These are real if $\omega^2 \geq 4(K(N^*,0)-P^* f_I(N^*,0))$ and thus the suspected minimum wavespeed is $\omega_{crit} = 2\sqrt{K(N^*,0)-P^* f_I(N^*,0)}$.

However, we need to check the other eigenvalues, namely of:

$$\begin{pmatrix} 0 & 1 & 0 & 0 \\ -\pi & -\omega & 1 & 0 \\ 0 & 0 & 0 & 1 \\ \frac{-P^*}{D_P}\left(\frac{\partial f}{\partial N}(N^*,0) + F_S\pi\right) & \frac{-F_S\omega P^*}{D_P} & \frac{F_S P^*}{D_P} & \frac{-\omega}{D_P} \end{pmatrix} \tag{22}$$

where $\pi = g(N^*) - cN^* - P^* \frac{\partial f}{\partial N}(N^*,0)$. The eigenvalues of this system are difficult to find given this is a quartic equation. However, they do not need to be real as they represent the predator–prey subsystem and spiraling around the predator–prey steady state poses no threat of negative populations. Thus we do not have any more restrictions on the values for ω.

However, if we assume that $F_S = 0$ and $D_P = 1$, then the characteristic equation can be reduced from a quartic to a quadratic equation: $\tau^2 + \pi\tau + P^* \frac{\partial f}{\partial N}(N^*,0)$, where $\tau = \lambda(\lambda+\omega)$ and $\pi = g(N^*) - cN^* - P^* \frac{\partial f}{\partial N}(N^*,0) < 0$. From this, we have $\tau = \frac{-\pi \pm \sqrt{\pi^2 - 4P^* \frac{\partial f}{\partial N}(N^*,0)}}{2}$. Thus we have $\lambda = \frac{-\omega \pm \sqrt{\omega^2 + 4\tau}}{2}$. Since $\pi < 0$ and $\frac{\partial f}{\partial N}(N^*,0) > 0$, then all eigenvalues are real if and only if τ is real, i.e. $\pi^2 > 4P^* \frac{\partial f}{\partial N}(N^*,0)$. This condition is the same as the condition for the predator–prey steady state to be stable. The eigenvalues for other values of F_S and D_P have not been found.

A.2 Summary and Conclusions

To summarise the previous calculations, the analytical minimum wavespeeds are:

- Predator invasion in the absence of infected prey:

  $\omega_{crit} = 2\sqrt{D_P(f(N^*,0)-1)}$, where N^* is the density of prey at the disease-free prey-only steady state.
- Predator invasion in the presence of infected prey:

  $\omega_{crit} = 2\sqrt{D_P(f(N^*,I^*)-1)}$, where N^* and I^* are the densities of the total prey and infected prey at the endemic prey-only steady state, respectively.
- Disease invasion in the presence of predators:

  $\omega_{crit} = 2\sqrt{K(N^*,0)-P^* f_I(N^*,0)}$, where N^* and P^* are the densities of the prey and predator at the disease-free prey–predator steady state, respectively.

B Numerical methods

The initial condition consists of two parts. First, there are the native specie(s), which we assume will be at the relevant (stable, at least in a non-spatial sense) coexistent steady state. The predator–prey and endemic prey steady state initial conditions are derived by running MATLAB's 'ode45' and taking their densities at the final time ($t = 1000$). The invading initial condition will generally be a step function of 0.1 for $x \leq 20$ and zero otherwise. However, for some scenarios, in particular when predator diffusion is very small (or zero), it is preferable for a smooth initial condition to be used. In these cases, a smooth approximation of the step function, $0.05(1-\tanh(x-20))$, is used.

The numerical scheme can be written as follows:

$$N(x,t+t_{step}) = N(x,t) + N_{growth}(x,(t,t+t_{step})) + N_{diffusion}(x,(t,t+t_{step})), \tag{23}$$

$$I(x,t+t_{step}) = I(x,t) + I_{growth}(x,(t,t+t_{step})) + I_{diffusion}(x,(t,t+t_{step})), \tag{24}$$

$$\begin{aligned} P(x,t+t_{step}) = P(x,t) + P_{growth}(x,(t,t+t_{step})) + P_{diffusion}(x,(t,t+t_{step}))... \\ ... + P_{taxis}(x,(t,t+t_{step})). \end{aligned} \tag{25}$$

where, for example $N_{growth}(x,(t,t+t_{step}))$, is the growth of N at point x over the time interval $(t,t+t_{step})$.

However, each of these terms have different properties. In particular, using one numerical scheme to deal with all these simultaneously would be highly problematic. In particular, the diffusion terms suggest using a scheme appropriate for parabolic PDEs, but such schemes would have real difficulty handling the taxis terms. Instead of trying to use one scheme to solve the whole system simultaneously, we will split the system into a sequence of smaller problems using a Strang splitting scheme (Chapter 18 of LeVeque, 1992; Tyson et al, 2000). This scheme is implemented as follows.

First, solve the diffusion only problem numerically for half a time step and take this as the new solution at time t, i.e. for predators we have:

$$P^*(x,t) := P(x,t+0.5*t_{step}) = P(x,t) + P_{diffusion}(x,(t,t+0.5t_{step})) \tag{26}$$

Do the same for susceptible and infected prey to derive $N^*(x,t)$ and $I^*(x,t)$, respectively. Following this, we then perform a taxis half step using an appropriate numerical scheme to again get a new solution at time t (note, this step only changes the predators since there is no taxis in the other classes).

$$P'(x,t) := P^*(x,t+0.5t_{step}) = P^*(x,t) + P_{taxis}(x,(t,t+0.5t_{step})) \tag{27}$$

The next step is to take a full time step with only the growth dynamics, using an appropriate solver. This will form a new solution, which will be centered at time $t+0.5t_{step}$.

$$\hat{P}(x,t+0.5t_{step}) := P'(x,t+t_{step}) = P'(x,t) + P_{growth}(x,(t,t+t_{step})) \tag{28}$$

Likewise, we get $\hat{N}(x,t+0.5t_{step})$ and $\hat{I}(x,t+0.5t_{step})$ by the same method, using $N'(x,t)$ and $I'(x,t)$ instead, respectively. Next, another taxis half step is taken (which only affects the predator equation). This gives a new solution at time $t+0.5t_{step}$.

$$\bar{P}(x,t+0.5t_{step}) := \hat{P}(x,t+t_{step}) = \hat{P}(x,t) + P_{taxis}(x,(t+0.5t_{step},t+t_{step})) \tag{29}$$

Finally, we take this solution and incorporate a half step of diffusion to get a final solution for time $t+t_{step}$.

$$P(x,t+t_{step}) := \bar{P}(x,t+0.5t_{step}) + P_{diffusion}(x,(t+0.5t_{step},t+t_{step})) \tag{30}$$

Do the same with $\hat{N}(x,t+0.5t_{step})$ and $\hat{I}(x,t+0.5t_{step})$ to get $N(x,t+t_{step})$ and $I(x,t+t_{step})$, respectively.

This scheme splits the problem into several smaller, more manageable steps, as well as allowing us to choose appropriate numerical methods for each subproblem instead of trying to use one scheme that would have difficulty handling the whole. One key advantage of this scheme is that it is of order 2 with respect to time and unconditionally stable as long as each subproblem is order 2 or higher.

For the growth step, the dynamics are local and thus a simple explicit ODEs solver can be used. We used the midpoint method (2nd order Runge–Kutta). This is a reliable scheme for ODE, and because of this, it was chosen for the full step. For diffusion, both a forward-time–centered-space (FTCS) scheme and a Crank–Nicolson scheme were used and compared. The former is of order 1 with respect to time (order 2 with respect to space). This scheme is conditionally stable; it is stable if $\frac{t_{step}}{(x_{step})^2} < 0.5$. The latter scheme is implicit and of order two with respect to time and space. It is unconditionally stable, although there are still numerical issues about artificial oscillations during the first few steps if $\frac{t_{step}}{(x_{step})^2}$ is too large and initial condition is too spiky. Consequently, the same step sizes will be used for both FTCS and Crank–Nicolson. Results between the two schemes have been compared and agree very well, the only visible difference being around $x = 0$ in some cases of spatiotemporal chaos. There are no noticeable differences with respect to the wavespeed and the wavefront.

For the taxis term, we have used a two-step Lax–Wendroff scheme. It is an explicit second order (with respect to both time and space) scheme for hyperbolic PDEs (Chapter 11 of LeVeque, 1992; Morton and Mayers, 2002). It is very good at following suitably smooth solutions, but has issues around very large gradients and discontinuities, where solutions will overshoot and oscillate around sharp (i.e. non-smooth) points, particularly behind the discontinuity. These oscillations dampen away from the discontinuity. This can lead to issues in a few cases, especially if this results in negative populations. However, this scheme does follow the magnitude of peaks and their wavespeed very well, two key aspects to our exploration of travelling waves. Note that this issue only really matters if repulsive preytaxis is too strong compared to diffusion in predators. In particular, if $D_P = 0$, then the numerical scheme breaks down for any repulsive preytaxis as negative populations arise. Other numerical schemes were considered. For example, an upwind scheme was considered, but it is only of order 1 in time and space. It does not exhibit these oscillations around sharp

points, but instead these points are smeared over as if there was some strong diffusive force, an effect that is undesirable as it would artificially flatten the wavefront, reducing prey gradients and thus reduce the strength of preytaxis. Another second order scheme is Beam–Warming, which is like the Lax–Wendroff scheme except the oscillations are ahead of the wave (LeVeque, 1992, Chapter 11). This potentially alters the dynamics ahead of the wave and may lead to negative populations in cases of attractive preytaxis. Likewise, the leapfrog scheme is of order two, but it has oscillations behind the wave that do not die out (Morton and Mayers, 2002). These oscillations are generic for second order schemes (LeVeque, 1992, Chapter 11).

It is well worth noting that the inclusion of predator diffusion increases the smoothness of the numerical solutions, which improves the reliability of the Lax–Wendroff scheme. This is why the step function is used for every simulation where $D_P > 0$. However, in the absence of predator diffusion, Figure 13(a) shows that the step function initial condition does not smooth out straight away but instead brings in damped oscillations/spikiness just behind the wavefront. This contrasts with Figure 3(a), where a smooth wave forms. However, even by $t = 5$, the solution in Figure 13(a) is largely smooth for the predator, that the oscillations and spikiness have largely gone. In fact, both Figure 3(b) and 13(b) show that the wave moves at the same speed (actually, in Figure 13(a) the travelling wave stays about 0.25 spatial units behind Figure 3(b) over times $t = 5, 10, 20, 50$ and 100, this difference can be explained by the time taken to converge to the wavefront). However, without diffusion, even the slightest repulsive preytaxis results in negative predator populations around the discontinuity in the initial condition and the eventual breakdown of the numerical solution with Lax–Wendroff; in such cases, a Beam–Weaming scheme should be used instead as it would behave like Lax–Wendroff does in Figure 13.

Boundary conditions are incorporated by setting the first and last spatial point to be equal to their immediate neighbour (and thus there is zero flux). This is done after each substep.

All simulations have step sizes of $t_{step} = 0.0005$ and $x_{step} = 0.05$ for time and space, respectively (unless stated otherwise). These step sizes satisfy stability conditions for the diffusion step as both FTCS and Crank-Nicolson because $\frac{t_{step}}{(x_{step})^2} = 0.2 < 0.5$ (in fact, it probably is 0.1 due to the half steps). Other time and space step sizes have been considered and results do not look different as long as they are sufficiently small and the condition $\frac{t_{step}}{(x_{step})^2} < 0.5$ is satisfied; in particular, the values for t_{step} and x_{step} in Figure 4 give results that look identical to the default step sizes. This all suggests that the results in this paper are robust and a consequence of the system and not numerical artifacts.

Overall, the use of a Strang splitting scheme allows the full model to be split into a sequence of smaller models, which individually can be solved with well-established methods. Although there are some issues around a discontinuous initial condition for the taxis step, these issues are negligible with sufficient levels of diffusion for predators, and only seem to provide major inaccuracies when repulsive preytaxis is high and diffusion very small (in which case, the Beam–Weaming scheme is more appropriate).

C Non-constant steady states of the spatio-temporal predator–prey system

The purpose of this section is to demonstrate that attractive (repulsive) preytaxis has a (de)stabilising effect on constant steady states for the predator–prey system.

If we suppose that there is a (spatially varying) perturbation of the form $(N', P') \propto \exp(i\sigma x + \lambda t)$ around the constant co-existent predator– prey steady steady (N^*, P^*). Then the Jacobian is:

$$J = \begin{pmatrix} -\sigma^2 + (g(N^*) - cN^* - P^* \frac{\partial f(N^*,0)}{\partial N}) & -1 \\ F_S\sigma^2 + P^* \frac{\partial f(N^*,0)}{\partial N} & -D_P\sigma^2 \end{pmatrix} \tag{31}$$

For this Jacobian, it has eigenvalues, λ that satisfy:

$$\lambda^2 - trace(J)\lambda + \det(J) = 0. \tag{32}$$

Now, $trace(J) = -(1+D_P)\sigma^2 + (g(N^*) - cN^* - P^* \frac{\partial f(N^*,0)}{\partial N})$. A condition for stability would be that this is negative. If we assume that the steady state is stable in the absence of spatial effects, then $g(N^*) - cN^* - P^* \frac{\partial f(N^*,0)}{\partial N} < 0$, then $trace(J) < 0$ for all σ.

Additionally, $\det(J) = D_P\sigma^2(\sigma^2 - (g(N^*) - cN^* - P^* \frac{\partial f(N^*,0)}{\partial N})) + F_S\sigma^2 + P^* \frac{\partial f(N^*,0)}{\partial N}$. Given $trace(J) < 0$, instability could occur if $\det(J) < 0$ for some $\sigma^2 > 0$, which is equivalent to there being a positive root (with respect to σ^2) of $\det(J) = 0$. Now, given $P^* \frac{\partial f(N^*,0)}{\partial N} > 0$, both roots are of the same sign (and distinct), which means that these roots are positive (and thus instability can occur) if and only if $F_S < D_P(g(N^*) - cN^* - P^* \frac{\partial f(N^*,0)}{\partial N})$. However, $g(N^*) - cN^* - P^* \frac{\partial f(N^*,0)}{\partial N}$ is negative as a consequence of assuming a stable (non-spatial) steady state, meaning that the preytaxis has to be sufficiently repulsive ($F_S << 0$) for instability to occur. Likewise, we can also conclude that attractive preytaxis ($F_S > 0$) has a stabilising effect.

References

Ainseba BE, Bendahmane M, Noussair A (2008) A reaction–diffusion system modeling predator–prey with prey-taxis. Nonlinear Analysis: Real World Applications 9:2086–2105

Arditi R, Tyutyunov Y, Morgulis A, Govorukhin V, Senina I (2001) Directed movement of predators and the emergence of density-dependence in predator–prey models. Theoretical Population Biology 59:207–221

Armstrong RA, McGehee R (1980) Competitive exclusion. American Naturalist 115:151–170

Aronson DG, Weinberger HF (1975) Multidimensional nonlinear diffusion arising in population genetics. In: Goldstein EA (ed) Partial differential equations and related topics, Lecture Notes in Mathematics, vol 446, Springer-Verlag, Berlin, pp 5–49

Aronson DG, Weinberger HF (1978) Multidimensional nonlinear diffusion arising in population genetics. Advances in Mathematics 30:38–76

Bate AM, Hilker FM (2013a) Complex dynamics in an eco-epidemiological model. Bulletin of Mathematical Biology 75:2059–2078

Bate AM, Hilker FM (2013b) Predator–prey oscillations can shift when dieases become endemic. Journal of Theoretical Biology 316:1–8

Bate AM, Hilker FM (2014) Disease in group-defending prey can benefit predators. Theoretical Ecology 7:87–100

Begon M, Townsend CR, Harper JL (2002) Ecology, 4th edn. Blackwell Publishing, Oxford

Bell SS, White A, Sherratt JA, Boots M (2009) Invading with biological weapons: the role of shared disease in ecological invasion. Theoretical Ecology 2:53–66

Berdoy M, Webster JP, Macdonald DW (2000) Fatal attraction in rates infected with toxoplasma gondii. Proceedings of the Royal Society London B 267:1591–1594

Berleman JE, Scott J, Chumley T, Kirby JR (2008) Predataxis behavior in Myxococcus xanthus. Proceedings of the National Academy of Sciences 105:17,127–17,132

Britton NF (2003) Essential Mathematical Biology. Springer, London

Chakraborty A, Singh M, Lucy D, Ridland P (2007) Predator–prey model with prey-taxis and diffusion. Mathematical and Computer Modelling 46:482–498

Coyner DF, Schaack SR, Spalding MG, Forrester DJ (2001) Altered predation susceptibility of mosquitofish infected with eustrongylides ignotus. Journal of Wildlife Disease 37:556–560

Curio E (1976) The ethology of predation, Zoophysiology and Ecology, vol 7. Spring-Verlag, Berlin

Dagbovie AS, Sherratt JS (2014) Absolute stability and dynamical stabilisation in predator–prey systems. Journal of Mathematical Biology 68:1403–1421

Dickman CR (1996) Impact of exotic generalist predators on the native fauna of Australia. Wildlife Biology 2:185–195

Dobson AP (1988) The population biology of parasite-induced changes in host behavior. The Quarterly Review of Biology 63:139–165

Edelstein-Keshet L (1988) Mathematical Models in Biology. Random House, New York

Errington PL (1946) Predation and vertebrate populations. The Quarterly Review of Biology 21:145–177

Ferreri L, Venturino E (2013) Cellular automata for contact ecoepidemic processes in predator–prey systems. Ecological Complexity 13:8–20

Freedman HI, Wolkowicz GSK (1986) Predator–prey systems with groups defence: the paradox of enrichment revisited. Bulletin of Mathematical Biology 48:493–508

Grünbaum D (1998) Using spatially explicit models to characterize foraging performance in heterogeneous landscapes. American Naturalist 151:97–115

Hardin G (1960) The competitive exclusion principle. Science 131:1292–1297

Hastings A (1996) Models of spatial spread: A synthesis. Biological Conservation 78:143–148

Hilker FM, Schmitz K (2008) Disease-induced stabilization of predator–prey oscillations. Journal of Theoretical Biology 255:299–306

Hilker FM, Malchow H, Langlais M, Petrovskii SV (2006) Oscillations and waves in a virally infected plankton system. Part II: Transition from lysogeny to lysis. Ecological Complexity 3:200–208

Hosono HG (1998) The minimal speed of traveling fronts for a diffusive Lotka–Volterra competition model. Bulletin of Mathematical Biology 60:435–448

Hudson PJ, Dobson AP, Newborn D (1992) Do parasites make prey vulnerable to predation? Red grouse and parasites. Journal of Animal Ecology 61:681–692

Johnson CG (1967) International dispersal of insects and insect-borne viruses. Netherlands Journal of Plant Pathology 1:21–43

Kareiva P, Odell G (1987) Swarms of predators exhibit ”preytaxis” if individual predators use area-restricted search. American Naturalist 130:233–270

Keller EF, Segel LA (1971) Traveling band of chemotactic bacteria: A theoretical analysis. Journal of Theoretical Biology 130:235–248

Krause J, Ruxton GD (2002) Living in Groups. Oxford University Press

Kubanek J (2009) Chemical defense in invertebrates. In: Hardege JD (ed) Chemical Ecology, EOLSS, Oxford, UK

Lafferty KD (1992) Foraging on prey that are modified by parasites. American Naturalist 140:854–867

Langer WL (1964) The black death. Scientific American February:114–121

Lee JM, Hillen T, Lewis MA (2008) Continuous traveling waves for prey-taxis. Bulletin of Mathematical Biology 70:654–676

Lee JM, Hillen T, Lewis MA (2009) Pattern formation in prey-taxis systems. Journal of Biological Dynamics 3:551–573

LeVeque RJ (1992) Numerical Methods for Conservation Laws. Birkhäuser, Basel

Lewis MA, Li B, Weinberger HF (2002) Spreading speed and linear determinacy for two-species competition models. Journal of Mathematical Biology 45:219–233

Lloyd HG (1983) Past and present distribution of red and grey squirrels. Mammal Review 13:69–80

Malchow H, Hilker FM, Petrovskii SV, Brauer K (2004) Oscillations and waves in a virally infected plankton system. Part I: The lysogenic stage. Ecological Complexity 1:211–223

Malchow H, Hilker FM, Sarkar RR, Brauer K (2005) Spatiotemporal patterns in an excitable plankton system with lysogenic viral infection. Mathematical and Computer Modelling 42:1035–1048

Malchow H, Petrovskii SV, Venturino E (2008) Spatiotemporal Patterns in Ecology and Epidemiology: Theory, Models, and Simulation. Chapman and Hall/CRC, New York

Middleton AD (1930) Ecology of the American gray squirrel in the British Isles. Proceedings of the Zoological Society London 2:809–843

Moore J (2002) Parasites and the behavior of animals. Oxford Series in Ecology and Evolution, Oxford University Press, Oxford

Morton KW, Mayers DF (2002) Numerical Solution of Partial Differential Equations. Cambridge University Press, Cambridge

Murray JD (2002) Mathematical Biology I: An Introduction. Third Edition, 3rd edn. Springer, New York

Murray JD (2003) Mathematical Biology II: Spatial Models and Biomedical Applications, 3rd edn. Springer, New York

Packer C, Holy RD, Hudson PJ, Lafferty KD, Dobson AP (2003) Keeping the herds healthy and alert: implications of predator control for infectious disease. Ecology Letters 6:797–802

Petrovskii SV, Li BL (2006) Exactly Solvable Models of Biological Invasion. Chapman and Hall/CRC, Boca Raton, Florida

Petrovskii SV, Malchow H (2000) Critical phenomena in plankton communities: KISS model revisited. Nonlinear Analysis: Real World Applications 1:37–51

Roy P, Upadhyay RK (2015) Conserving Iberian Lynx in Europe: Issues and challenges. Ecological Complexity 22:16–31

Sapoukhina N, Tyutyunov Y, Arditi R (2003) The role of prey taxis in biological control: A spatial theoretical model. American Naturalist 162:61–76

Sherratt JS, Dagbovie AS, Hilker FM (2014) A mathematical biologist's guide to absolute and convective instability. Bulletin of Mathematical Biology 76:1–26

Shigesada N, Kawasaki K (1997) Biological Invasions: Theory and Practice. Oxford University Press, Oxford

Sieber M, Hilker FM (2011) Prey, predators, parasites: intraguild predation or simpler community models in disguise? Journal of Animal Ecology 80:414–421

Sieber M, Malchow H, Schimansky-Geier L (2007) Constructive effects of environmental noise in an excitable prey–predator plankton system with infected prey. Ecological Complexity 4:223–233

Siekmann I, Malchow H, Venturino E (2008) Predation may defeat spatial spread of infection. Journal of Biological Dynamics 2:40–54

Skellam JG (1951) Random dispersal in theoretical populations. Biometrika 38:196–218

Slobodkin LB (1968) How to be a predator. American Zoologist 8:43–51

Su M, Hui C (2011) The effect of predation on the prevalence and aggregation of pathogens in prey. BioSystems 105:300–306

Su M, Hui C, Zhang YY, Li Z (2008) Spatiotemporal dynamics of the epidemic transmission in a predator–prey system. Bulletin of Mathematical Biology 70:2195–2210

Su M, Hui C, Zhang Y, Li Z (2009) How does the spatial structure of habitat loss affect the eco-epidemic dynamics? Ecological Modelling 220:51–59

Tompkins DM, White AR, Boots M (2003) Ecological replacement of native red squirrels by invasive greys driven by disease. Ecology Letters 6:189–196

Tyson R, Lubkin SR, Murray JD (1999) Model and analysis of chemotactic bacterial patterns in a liquid medium. Journal of Mathematical Biology 38:359–375

Tyson R, Stern LG, LeVeque RJ (2000) Fractional step methods applied to a chemotaxis model. Journal of Mathematical Biology 41:455–475

Tyutyunov YV, Titova LI, Senina IN (2017) Prey-taxis destabilizes homogeneous stationary state in spatial Gause-Kolmogorov-type model for predator–prey system. Ecological Complexity 31:170–180

Upadhyay RK, Roy P, Venkataraman C, Madzvamuse A (2016) Wave of chaos in a spatial eco-epidemiological system: Generating realistic patterns of patchiness in rabbit-lynx dynamics. Mathematical Biosciences 281:98–119

Vyas A, Kim S, Glacomini N, Boothroyd JC, Sapolsky RM (2007) Behavioral changes induced by toxoplasma infection of rodents are highly specific to aversion of cat odors. Proceedings of the National Academy of Sciences 104:6442–6447

Wang Q, Yang S (2017) Nonconstant positive steady states and pattern formation of 1D prey-taxis systems. Journal of Nonlinear Science 27:71–91

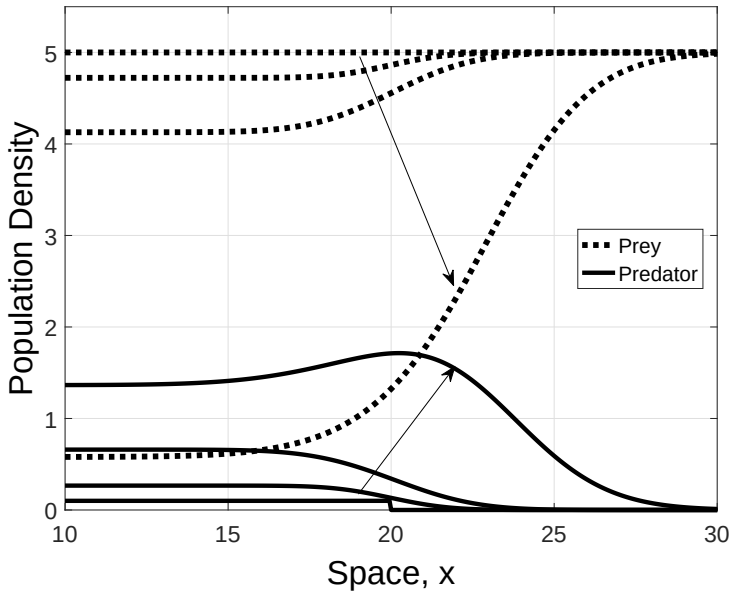

(a)

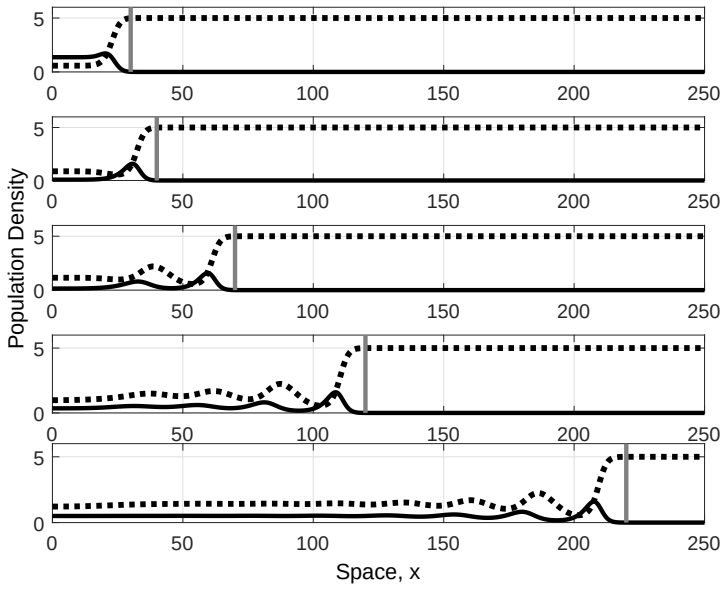

(b)

Fig. 1 Predator invasion in the absence of disease. No preytaxis. (a) shows the initial stages of predator invasion, where the predators grow locally up to steady state and spread to converge to the shape of the travelling wave. (b) shows that after this convergence, the wave travels with a speed that agrees with the analytic speed. For (a) the times are $T = 0, 1, 2, 5$ (shown in different curves) whereas for (b) the times are $T = 5, 10, 25, 50, 100$ (shown as different panels, from top to bottom). The dotted lines represent total prey density, whereas the bold lines represent predator density. The grey vertical lines in (b) represent the expected position of the wavefront according to the analytical wavespeed. Parameter values: $b = 1$, $m = 0.5$, $c = 0.1$, $h_S = 0.3$, $D_P = 1$ and $F_S = 0$.

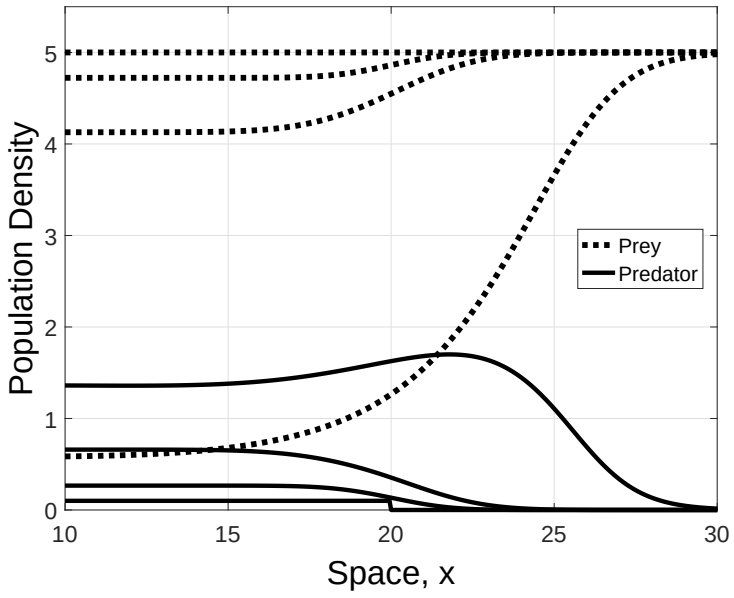

(a)

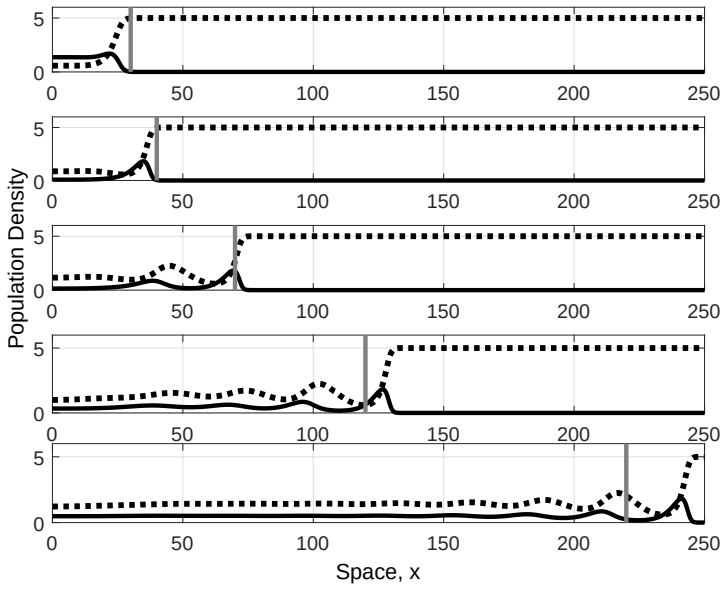

(b)

Fig. 2 Predator invasion in the absence of disease. Attractive preytaxis. (a) shows the initial stages of predator invasion, where the predators grow locally up to steady state and spread to converge to the shape of the travelling wave. (b) shows that after this convergence, the wave travels faster than the analytic speed. The times and lines used are the same as in Figure 1. Parameter values: Same as in Figure 1, except $F_S = 1$.

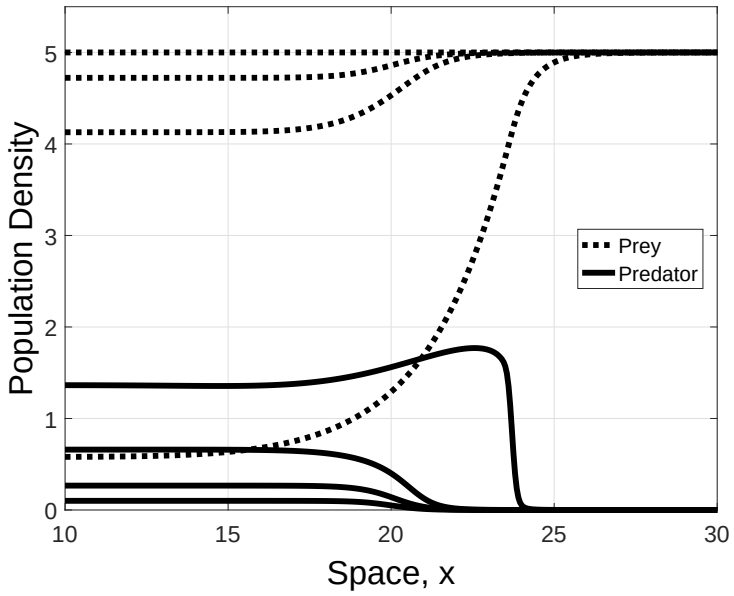

(a)

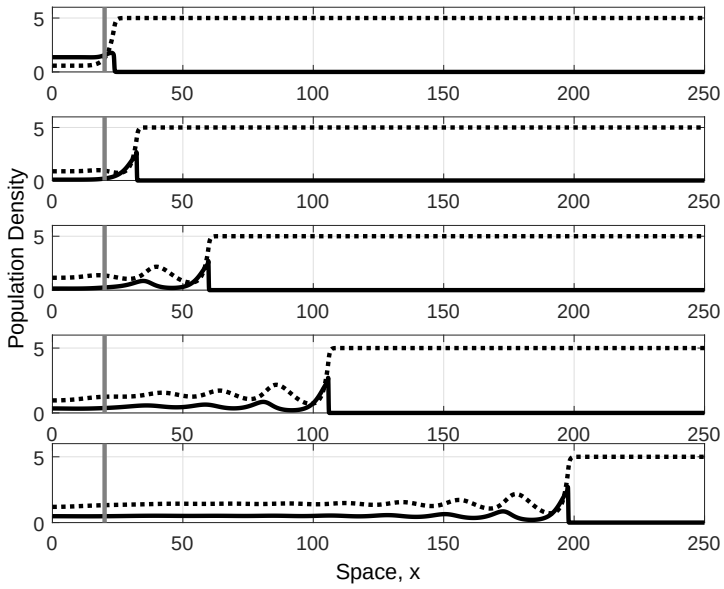

(b)

Fig. 3 Predator invasion in the absence of disease. Attractive preytaxis, no predator diffusion. (a) shows the initial stages of predator invasion, where the predators grow locally up to steady state and spread to converge to the shape of the travelling wave. (b) shows that after this convergence, the wave moves (at some wavespeed) where it should not in the absence of preytaxis. The times and lines used are the same as in Figure 1. Parameter values: Same as in Figure 1, except $F_S = 1$ and $D_P = 0$. The initial condition is a smoothed approximation of the step function $(0.05(1 - tanh(x - 20)))$. Results for the normal step function initial conditions are in Figure 13 (in Appendix).

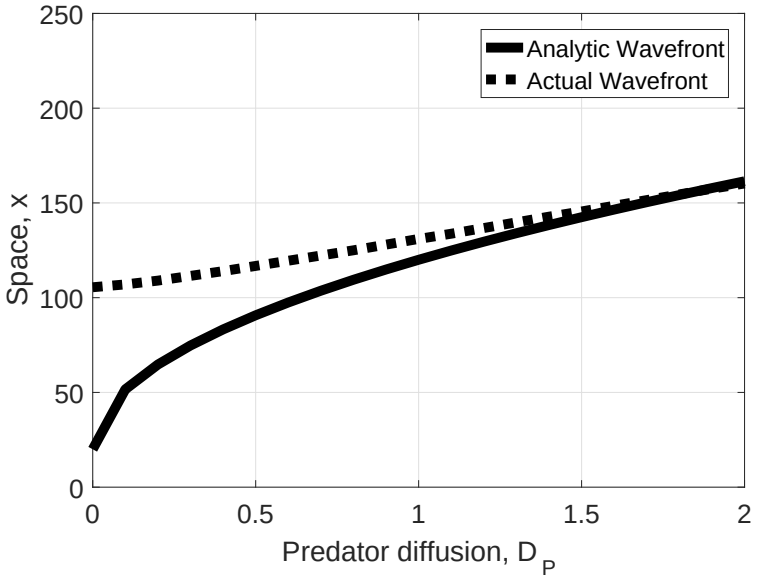

Fig. 4 Predator invasion in the absence of infected prey. Attractive preytaxis, various values of predator diffusion coefficient. Position of wavefront and analytic wavefront from the analytic minimum wavespeed after $t = 50$. We find that for low diffusion coefficients, attractive preytaxis leads to a large increase in wavespeed, whereas for larger diffusion coefficients predators have wavespeeds much closer to the analytic wavespeed. The wavefront is measured as the point in space where predator density is 0.1. Unlike other figures, the numerical solutions are for $t_{step} = 0.005$ and $x_{step} = 0.1$. Note that $D_P = 0$ and $D_P = 1$ correspond to the fourth panels of Figures 3(b)/13(b) and 2(b), respectively. Parameter values: Other than the varying D_P, the same as in Figure 2.

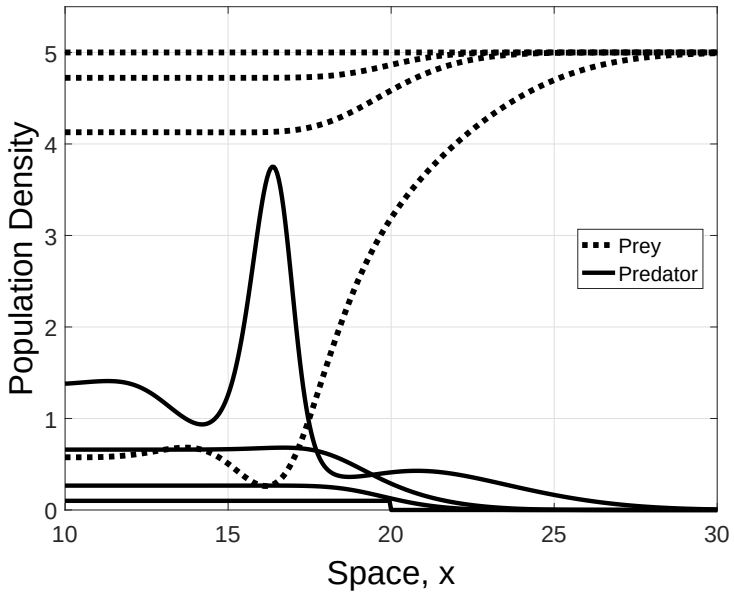

(a)

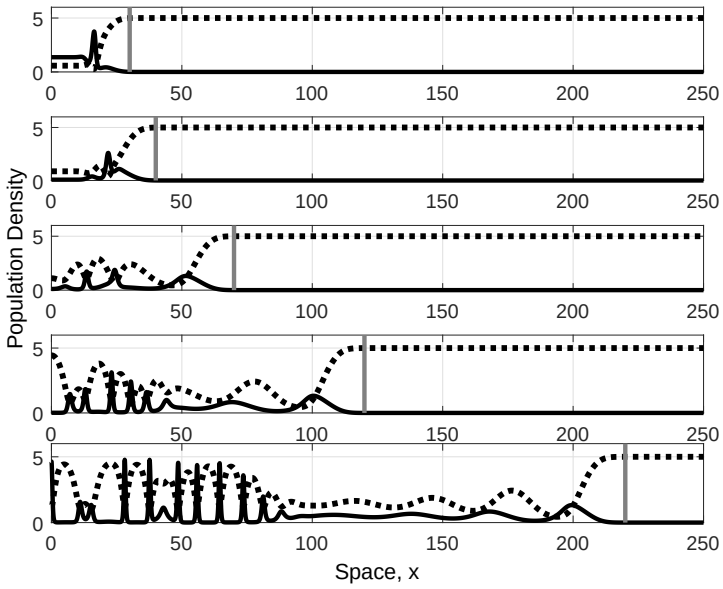

(b)

Fig. 5 Predator invasion in the absence of disease. Repulsive preytaxis. (a) shows the initial stages of predator invasion, where the predators grows locally up to steady state and spread to converge to the shape of the travelling wave. (b) shows that after this convergence, the wave travels with a speed that agrees with the analytic speed. The times and lines used are the same as in Figure 1. Parameter values: Same as in Figure 1, except $F_S = -3$.

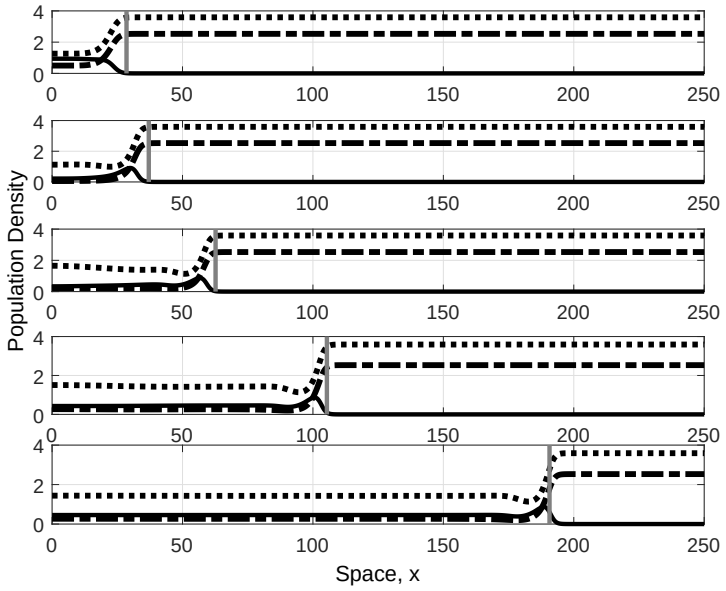

(a)

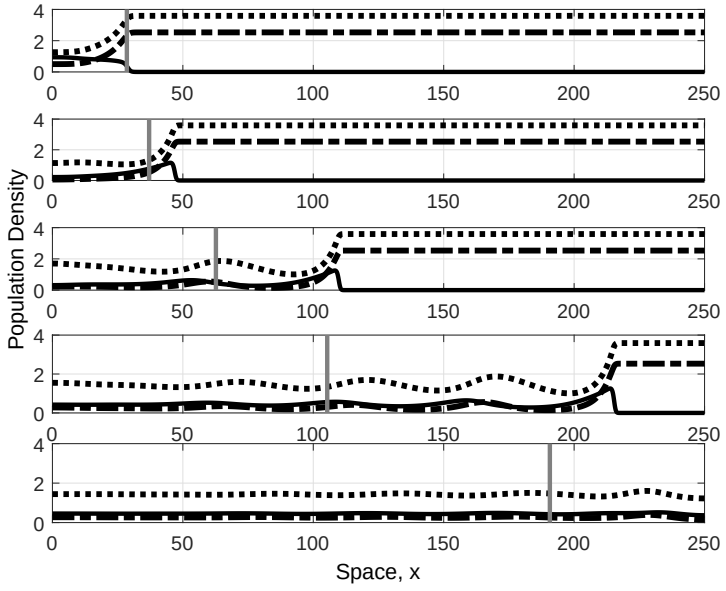

(b)

Fig. 6 Predator wave invading an endemic prey-only steady state. Predators are attracted to (a) susceptible prey ($F_S = 10$, $F_I = 0$) and (b) infected prey ($F_S = 0$, $F_I = 10$). In (a) the predator wave is marginally faster than the analytic wavespeed, whereas in (b) the predator wave is much faster than the analytic wavespeed. The dotted lines represent total prey density, the bold lines represent predator density and the dash-dotted line represent infected prey. The times are (from top to bottom) $T = 5, 10, 25, 50, 100$. The grey vertical lines represent the expected position of the wavefront according to the analytical wavespeed. Other parameters: Same as in Figure 1, with additional parameters $\beta = 1$, $\mu = 0.2$, $h_I = 0.3$, $a_R = 1$ and $D_R = 1$.

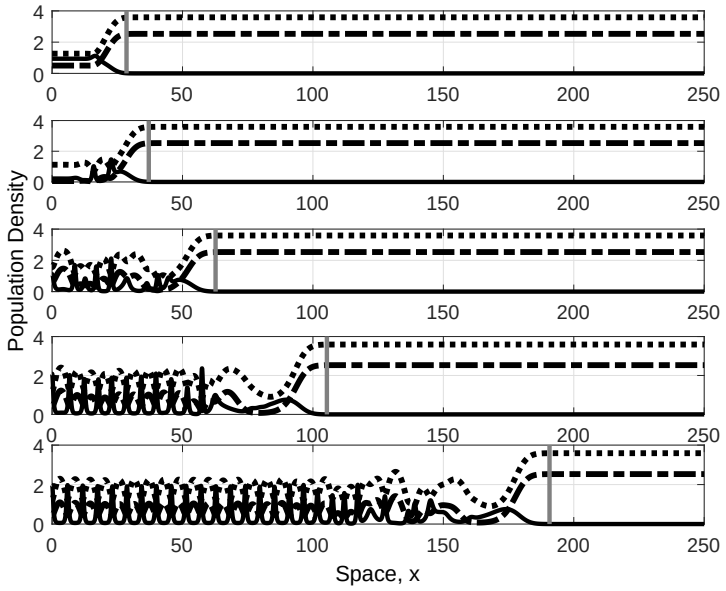

(a)

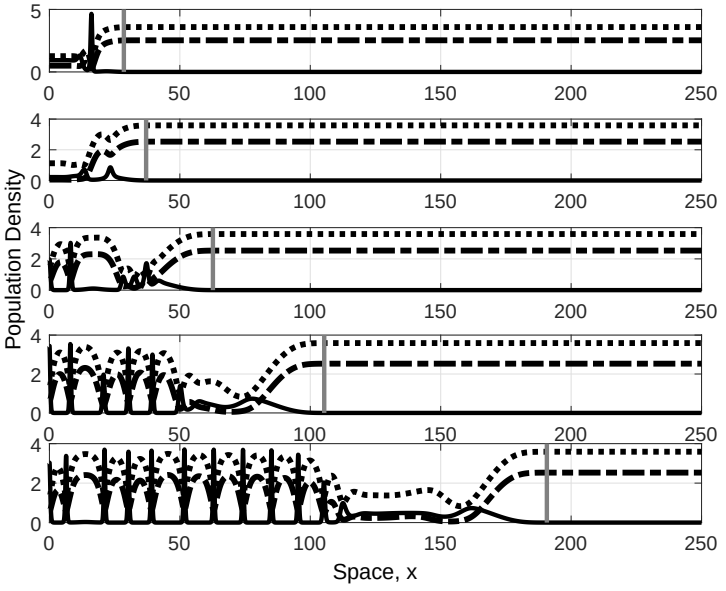

(b)

Fig. 7 Predator wave invading an endemic prey-only steady state. Predators are repelled by (a) susceptible prey ($F_S = -10$, $F_I = 0$) and (b) infected prey ($F_S = 0$, $F_I = -10$). Both (a) and (b) demonstrate that the predator wave spreads at the analytic wavespeed, and that spatiotemporal chaos or oscillations occur far behind the wavefront. Other parameters: Same as in Figure 6. The times and lines used are the same as in Figure 6.

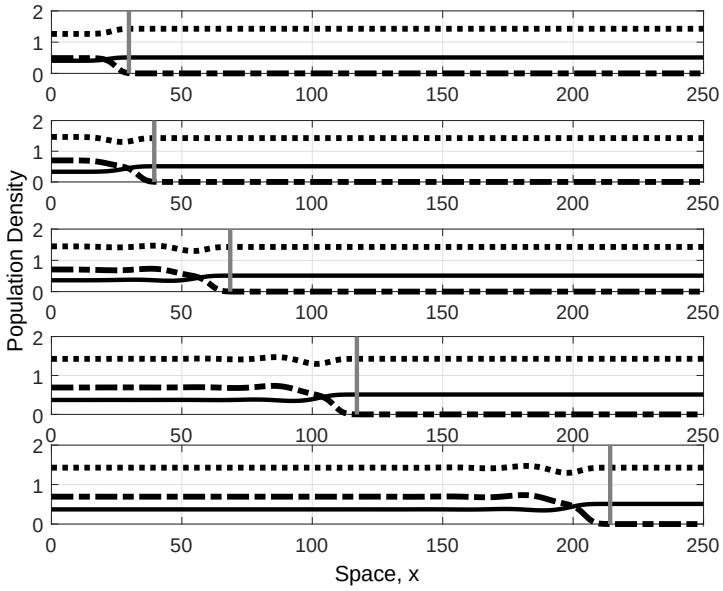

Fig. 8 Infection wave invading predator–prey steady state. No preytaxis. The disease spreads at the analytic wavespeed, which is represented by the vertical line, as before. The times and lines used are the same as in Figure 6. Parameter values: Same as in Figure 6 except $\beta = 1.5$.

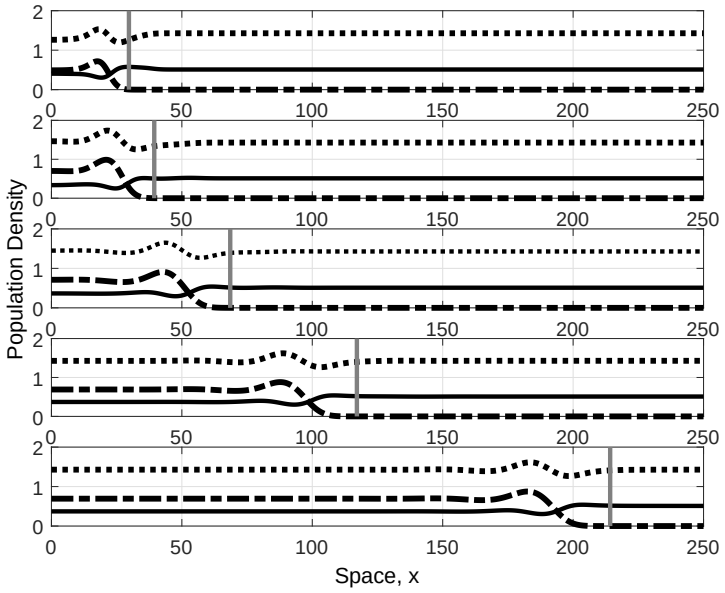

(a)

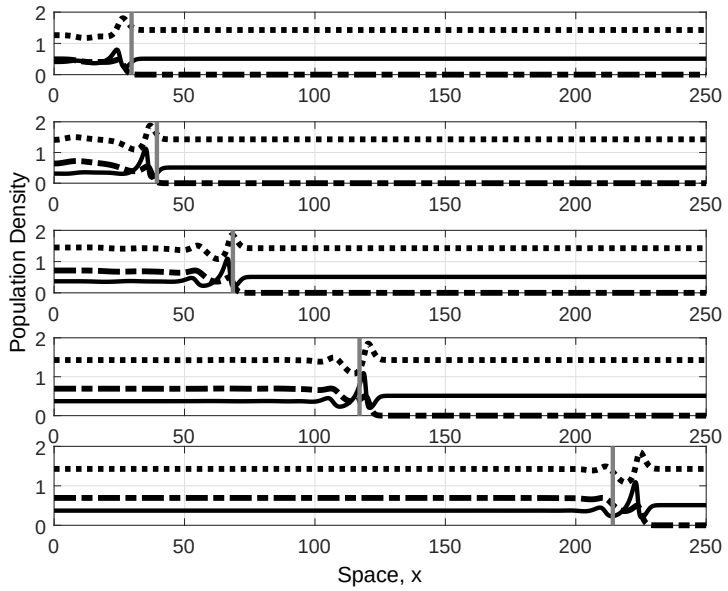

(b)

Fig. 9 Infection wave invading predator–prey steady state. (a) susceptible prey attract predators ($F_S > 0$), and (b) infected prey attract predators ($F_I > 0$). In (a), the infection wave moves at the analytic wavespeed, whereas in (b), the wavespeed is faster than the analytic wavespeed. The times and lines used are the same as in Figure 6. Parameter values (a) $F_S = 20$ and $F_I = 0$ and (b) $F_S = 0$ and $F_I = 20$. Other parameters: Same as in Figure 8.

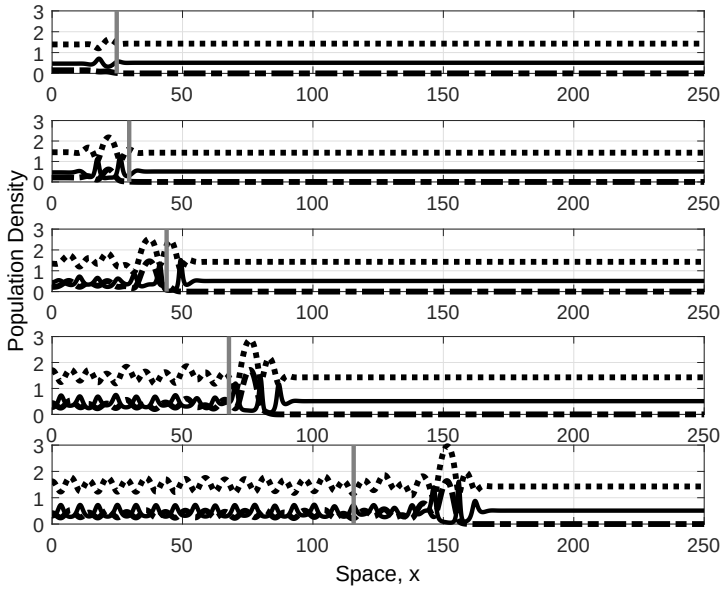

(a)

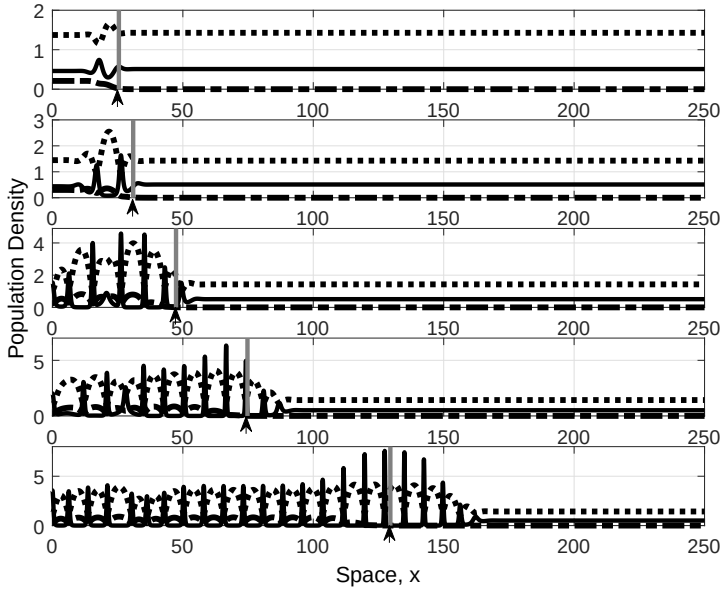

(b)

Fig. 10 Infection wave invading predator–prey steady state. Susceptible prey repel predators. Comparison of (a) density dependent and (b) frequency dependent transmission. In (a), the wave moves faster than the analytic wavespeed, whereas in (b) the wave moves at the same speed as the analytic wavespeed. The times and lines used are the same as Figure 6, with arrows added to (b) to emphasise the location of the grey line representing the expected position of the disease wavefront according to the analytic wavespeed. Parameter values (a) $\beta = 1$ and (b) $\beta_{FD} = 1.5$. Other parameters: Same as in Figure 8 except $F_S = -5$ and $F_I = 0$.

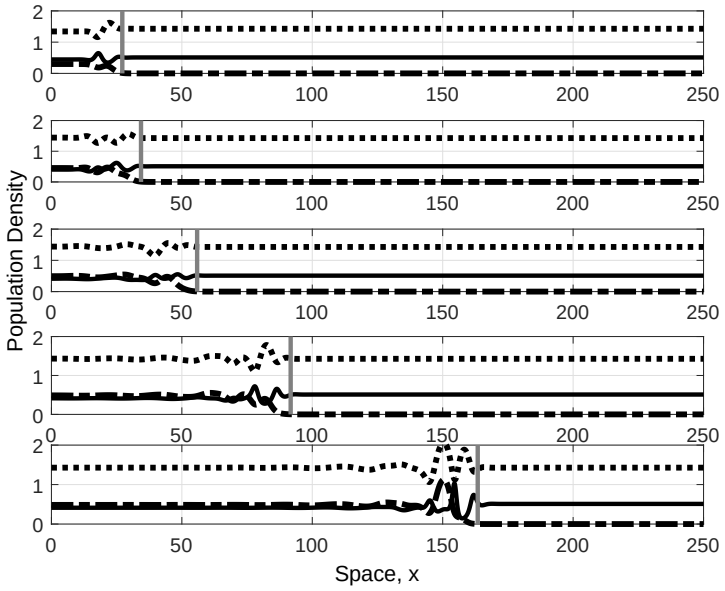

Fig. 11 Infection wave invading predator–prey steady state. Susceptible prey repel predators. Higher transmissibility than in Figure 10(a). The disease spreads at the analytic wavespeed. The times and lines used are the same as in Figure 6. Parameter values: $\beta = 1.2$, otherwise same as in Figure 8.

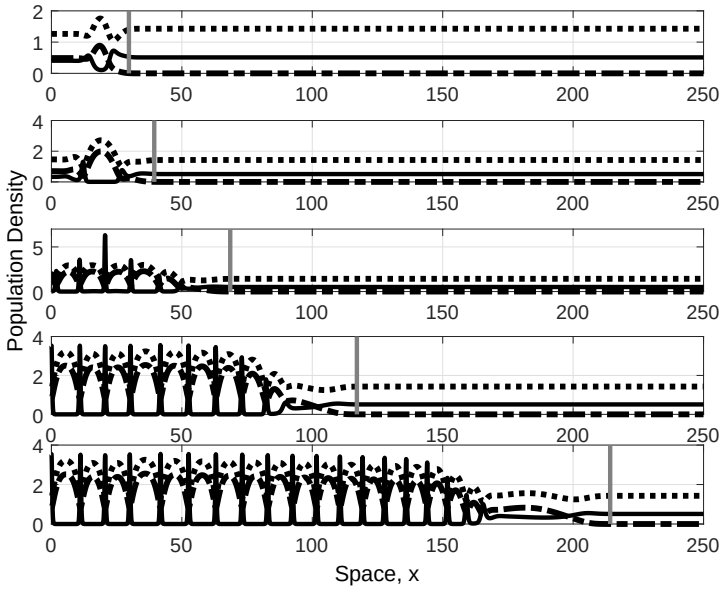

Fig. 12 Infection wave invading predator–prey steady state. Infected prey repel predators. The infection wave spreads at the same speed as the analytic wavespeed. Behind the wavefront the dynamics are oscillatory or chaotic. The times and lines used are the same as in Figure 6. Parameter values: Same as in Figure 8 except $F_S = 0$ and $F_I = -10$.

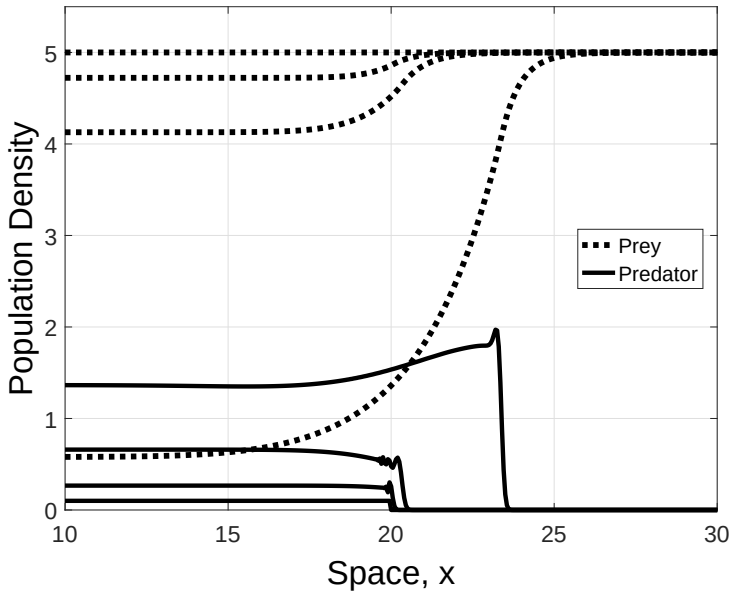

(a)

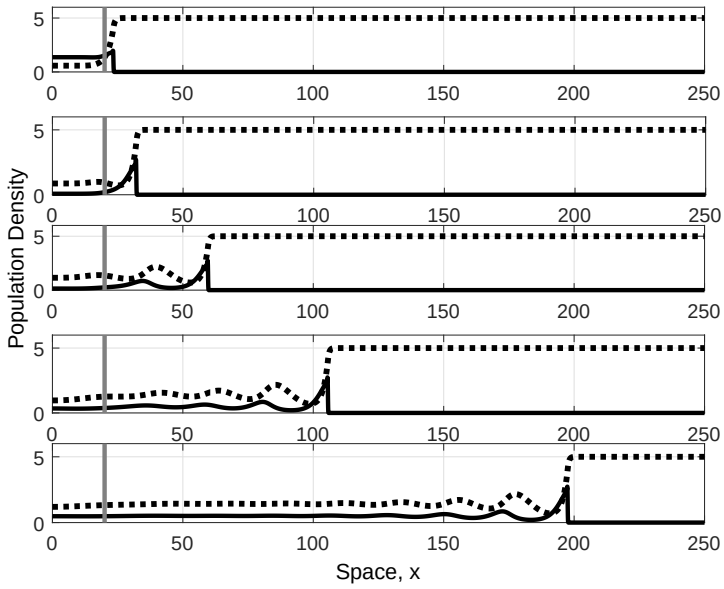

(b)

Fig. 13 Predator model. Attractive preytaxis, no predator diffusion. Step function as an initial condition (in contrast to Figure 3 which used a smooth approximation). Dampened 'spikiness' occurs directly behind the wave due to the use of Lax-Wendroff to simulate preytaxis. However, comparing with Figure 3, after some initial numerical issues around the discontinuity, the same travelling wave and wavespeed will eventually match, suggesting the numerical issue have little to no bearing on the long term dynamics.